Design of Simple Steel Connections under Fire Temperatures

ELIE G. HANTOUCHE, KARIM K. AL KHATIB, and HAGOP V. JABOTIAN

ABSTRACT

A methodology is developed for designing simple steel connections (shear tab and double angle) subjected to fire. The proposed methodology is based on quantifying the strength and stiffness of steel framed simple connections at elevated temperatures. To achieve this, first, a stiffness-based model that characterizes the rotational stiffness of simple steel connections when subjected to fire temperatures is developed. The model is capable of predicting the behavior of two widely used simple steel connections (shear tab and double angle) when subjected to fire temperatures. It incorporates the connection rotation of key component elements and the nonlinear behavior of both bolts and base materials at elevated temperatures. The model is validated against experimental results available in the literature under steady-state temperature analysis. The model covers all possible limit states and governing failure modes under different loading and temperature conditions. It can be considered a practical tool for designing simple steel connections for professional structural fire engineers in the United States. Step-by-step design examples of simple steel connections in an isolated frame are provided to illustrate the incorporation of the developed stiffness model in a fire design procedure. The presented design procedure accounts for the additional load demand on the connection during fire. This includes the load demand due to thermal expansion and beam sagging.

Keywords: Stiffness-based model, steady-state temperature, fire, simple connections, fire design.

INTRODUCTION

Steel connections play an important role in maintaining the stability and integrity of steel building frames especially when exposed to fire temperatures. Failure of steel connections under fire loading can lead to total structural collapse. This was confirmed through the investigation of many fire disasters (Sunder, 2005) which reported that progressive structural collapse is mainly initiated by connection failure. In fire events, the behavior of steel connections is more complex due to geometrical and material nonlinearities. Almost no structural design guideline can be found that provides an adequate performance of steel connections in fire from a structural perspective. Instead, the available U.S. standards rely on the applied insulation to reduce the exposure of steel connections to fire temperatures, mitigating fire risks to an acceptable level.

Simple steel connections are extensively used in steel structures for their ease of use and low fabrication cost. The two commonly used simple steel connections in the United States are the shear tab and the double-angle connections. They are ideally designed as pin connections that resist shear forces resulting from gravity loads only. However, in fire events, these connections are subjected to higher load demands due to the thermal expansion and sagging of the steel beam, in addition to the degradation of the steel properties at high temperatures. Therefore, it is of paramount importance to find reliable and practical tools that can predict the changes in the stiffness and behavior of these connections at elevated temperatures. That is, understanding the behavior of steel connections in such severe conditions is necessary for the fire design of steel connections to prevent any structural instability.

Characterizing the connection performance and behavior at elevated temperatures forms the basis for fire design of steel connections. Experimental research programs have been conducted in the past few years to investigate the robustness of simple steel connections in fire (Hu and Engelhardt, 2012; University of Sheffield, 2007; Wald et al., 2006; Wang et al., 2011). Experimental work was conducted by Wald et al. (2006) to examine the global structural behavior of an eight-story composite steel–concrete building under fire. Two types of simple steel connections—flexible end plate and shear tab connections—were tested. The results showed that the structure did not lose its global stability when subjected to fire. Note that the beams and the connections were not protected against fire temperatures. Similar findings were observed in the experimental program conducted by

Elie G. Hantouche, Associate Professor, Department of Civil and Environmental Engineering, American University of Beirut, Beirut, Lebanon. Email: eh12@aub.edu.lb (corresponding)

Karim K. Al Khatib, Graduate Student, Department of Civil and Environmental Engineering, American University of Beirut, Beirut, Lebanon. Email: kka05@mail.aub.edu

Hagop V. Jabotian, Graduate Student, Department of Civil and Environmental Engineering, American University of Beirut, Beirut, Lebanon. Email: hvj00@mail.aub.edu

Paper No. 2018-11R

Wang et al. (2011) that investigated the robustness of different types of steel connections in restrained steel frames subjected to fire. The results showed that simple connections, specifically double angle, performed well in fire by providing high ductility and rotational capacity. The fire resilience of the double-angle connection, when subjected to thermally induced loading, was also experimentally tested by Pakala et al. (2012). Owing to its inherent rotational ductility, the double-angle connection was able to survive the fire test without experiencing any failure.

Numerical investigations were also conducted previously to study the behavior of simple steel connections under fire (Garlock and Selamet, 2010; Hantouche et al., 2016; Wuwer et al., 2012; Selamet and Garlock, 2010). Selamet and Garlock (2010) proposed, based on finite element (FE) studies, simple modifications on the shear tab connection detailing that improves the performance of such connections during fire scenarios. Furthermore, Hantouche et al. (2016) performed FE simulations to identify the key parameters affecting the behavior of double-angle connections at elevated temperatures. The results showed that the main factors affecting the connection behavior are load ratio, initial cooling temperature, location of the double angle, and gap distance. It was also concluded that double-angle connections have better performance at elevated temperatures when compared with shear tab connections. Seif et al. (2013; 2016) conducted an extensive numerical investigation to examine the effect of elevated temperature on simple shear tab connections. It was found that the change in failure modes is not only caused by the degradation of the steel material when subjected to fire, but also on the deformations that can be accommodated prior to fracture due to restraint thermal expansion or contraction. Over the past few years, several studies were conducted to develop mechanical (stiffness) models capable of predicting the load-deformation response of steel connections at ambient and elevated temperatures. As an example, Yu et al. (2009a; 2009b; 2009c) developed a mechanical (stiffness) model based on numerical and experimental studies for shear tab and double-angle connections under fire temperatures.

Previous studies showed that the survival of unprotected steel beams depends on the ability of the steel connections to withstand the additional fire loadings, especially at late stages of fire. Very limited research, however, focused on developing a design-oriented guideline that quantifies the load demand on simple steel connections under transient-state conditions of fire. To address this shortcoming, this study combines the characterization of simple steel connection behavior at elevated temperatures with fire design procedures. First, the study proposes a stiffness-based model that can be considered as a practical and simple tool to be used by structural fire designers. The proposed model is capable of predicting the overall rotational stiffness and strength of shear tab and double-angle connections under steady-state temperature conditions. The developed stiffness model is used in a step-by-step connection design procedure to predict the moment demand caused by the beam sagging in fire. Moreover, the additional fire loadings are incorporated in the calculation of stresses to reach a robust fire design of simple steel connections to withstand the fire temperatures.

STIFFNESS-BASED MODEL

A stiffness-based model is developed to predict the force-rotation characteristics of shear tab and double-angle connections at elevated temperatures. The proposed stiffness model consists of a series of linear and nonlinear springs that are combined together to predict the rotational stiffness and capacity of the whole connection. The following equations are based on ambient temperature formulations while considering the material properties as temperature-dependent. The retention factors incorporated in the stiffness-based model for steel materials, bolts, and welds are proposed by Lee et al. (2013), Hu et al. (2007), and Eurocode 3 (CEN, 2005a), respectively.

Joint Component Stiffness Coefficients

The stiffness coefficients of the springs that are incorporated in the proposed stiffness model are defined based on equations available in the literature. The stiffness components for each bolt row are presented below.

Web Angle in Bending

The stiffness of the web angle in bending, k_{ab}, is determined using this equation from Eurocode 3 (CEN, 2005b), Section 6.3.2:

$$k_{ab} = K_E E \frac{0.9 l_{eff,ab} t^3}{m^3} \tag{1}$$

where K_E is the temperature-dependent retention factor for the stiffness of the base materials; E is the elastic modulus of the steel material at ambient temperature; $l_{eff,ab}$ is the effective length of the double angles in bending in each bolt-row, using the same approach in calculating the effective length of the equivalent T-stub in bending as proposed by Eurocode 3 (CEN, 2005b); t is the thickness (of the angle leg); and m is the distance from the center of the bolt to the fillet of the angle leg.

Bolt in Tension

The stiffness of the bolt in tension, k_{bt}, can be calculated as proposed by Eurocode 3 (CEN, 2005b), Section 6.3.2:

$$k_{bt} = K_E E \frac{1.6 A_b}{L_b} \tag{2}$$

where A_b is the effective area of the bolt shank in tension, and L_b is the elongation length of the bolt shank, which consists of the grip length (thickness of material and washers) of the bolt and half the sum of the height of the bolt head and the height of the nut.

Beam Web/Angle Leg in Bearing

The stiffness of beam web or angle leg in bearing, k_{pb}, is taken from Eurocode 3 (CEN, 2005b), Section 6.3.2:

$$k_{pb} = 12 n_b k_b k_t d_b K_{ut} F_{ut} \tag{3}$$

where n_b is the number of bolt columns, while k_b and k_t are defined as:

$$k_b = \min\left\{0.25\frac{e_b}{d_b}+0.5;\ 0.25\frac{p_b}{d_b}+0.375;\ 1.25\right\} \tag{4}$$

$$k_t = \min\left\{1.5\frac{t}{d_{M16}};\ 2.5\right\} \tag{5}$$

where e_b is the distance from the bolt to the free edge of the plate in the direction of the load transfer, d_b is the diameter of the bolt shank, p_b is the spacing of the bolt in the direction of the load transfer, and d_{M16} is the diameter of an M16 bolt. K_{ut} is the temperature-dependent retention factor for the ultimate strength of the base material, and F_{ut} is the ultimate strength of the steel base material at ambient temperature.

Shear Tab Plate in Bearing

The bearing stiffness of the shear tab plate, k_{tb}, is computed using this equation from Yu et al. (2009b):

$$k_{tb} = \Omega t K_{yt} F_{yt}\left(\frac{d_b}{25.4}\right)^{0.8} \tag{6}$$

where Ω is a temperature-dependent parameter defined in Yu et al. (2009b), K_{yt} is the temperature-dependent retention factor for the yield strength of the steel base material, and F_{yt} is the material yield strength of the steel base material at ambient temperature.

Bolt in Shear

The shear bolt stiffness, k_{bs}, is defined in Wuwer et al. (2012) as:

$$k_{bs} = \frac{8 n_b d_b^2 K_{bt} F_{ub}}{d_{M16}} \tag{7}$$

where K_{bt} is the temperature-dependent retention factor for the bolt strength, and F_{ub} is the ultimate strength of the bolt material at ambient temperature.

Beam Flange in Contact with Column

The stiffness of the beam flange in contact with the column, k_{bcc}, is modeled using the axial stiffness of a beam element:

$$k_{bcc} = \frac{K_E E A_f}{L} \tag{8}$$

where A_f represents the effective area of the beam lower web and the beam bottom flange in contact with the face of the column, and L is the length of the beam. This spring is activated only when the beam comes in contact with the column after a specific degree of connection rotation.

Equivalent Stiffness of Simple Connections

The equivalent stiffness of the shear tab and double angle connections can be defined by assembling the stiffness of each component as presented in Figures 1(a) and 1(b), respectively. As seen in Figures 1(a) and 1(b), the equivalent stiffness of each of the shear tab and double-angle connections is presented by a group of bolt-rows composed of many component springs. The stiffness component of a single bolt-row of the shear tab connection can be expressed by:

$$\frac{1}{k_{bolt\ row}} = \frac{1}{k_{tb}} + \frac{1}{k_{bs}} + \frac{1}{k_{pb,beam}} \tag{9}$$

The stiffness component of a single bolt-row of the double angle connection can be expressed by:

$$\frac{1}{k_{bolt\ row}} = \frac{1}{k_{bt}} + \frac{1}{k_{ab}} + \frac{1}{k_{beam\text{-}angle\ lapjoint}} \tag{10}$$

where $k_{beam\text{-}angle\ lapjoint}$ represents the stiffness of a double-lap joint and is calculated by the following equation:

$$\frac{1}{k_{beam\text{-}angle\ lapjoint}} = \frac{2}{\left(\frac{1}{k_{pb,angle}} + \frac{1}{k_{bs}}\right)} + \frac{1}{k_{pb,beam}} \tag{11}$$

Rotational Stiffness of Simple Connections

To predict the connection rotation, the equivalent rotational stiffness of the connection, k_r, needs to be calculated and is defined as:

$$k_r = k_{bolt\ row} h^2 \tag{12}$$

where h is the distance between the end components connecting the shear tab plate or double-angle leg to the column, as shown in Figures 1(a) and 1(b), respectively. The connection rotation, θ_c, of the shear tab or double-angle connections can be calculated as follows:

$$\theta_c = \frac{M}{k_r} \tag{13}$$

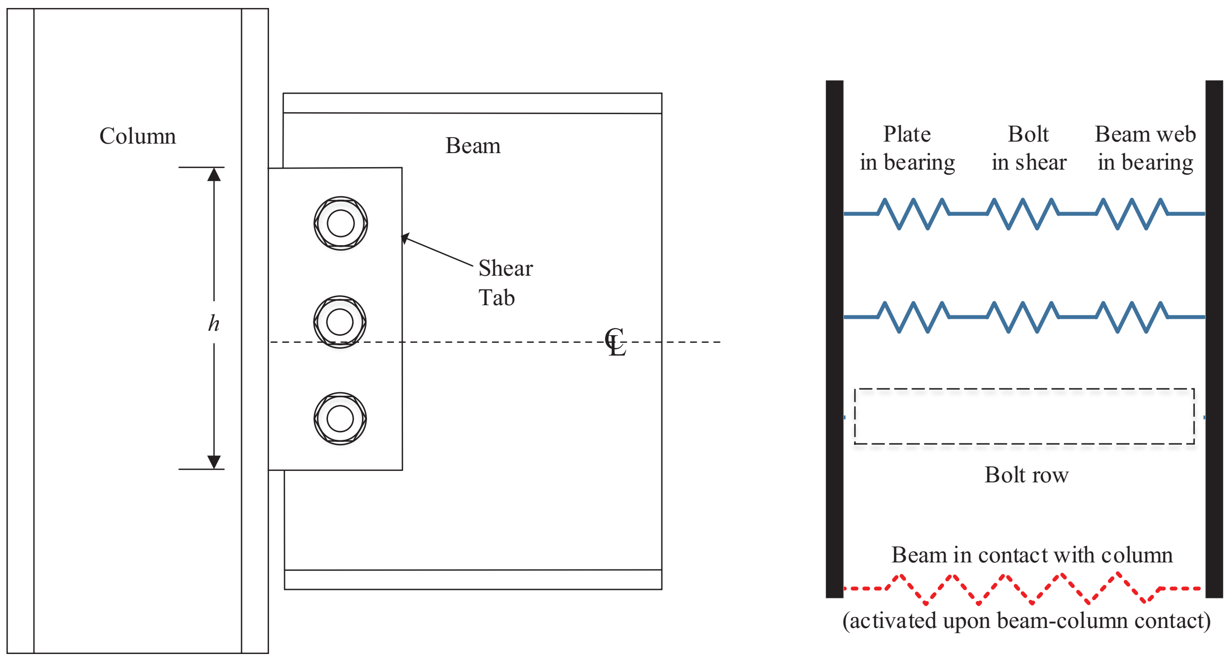

(a) Shear tab connection

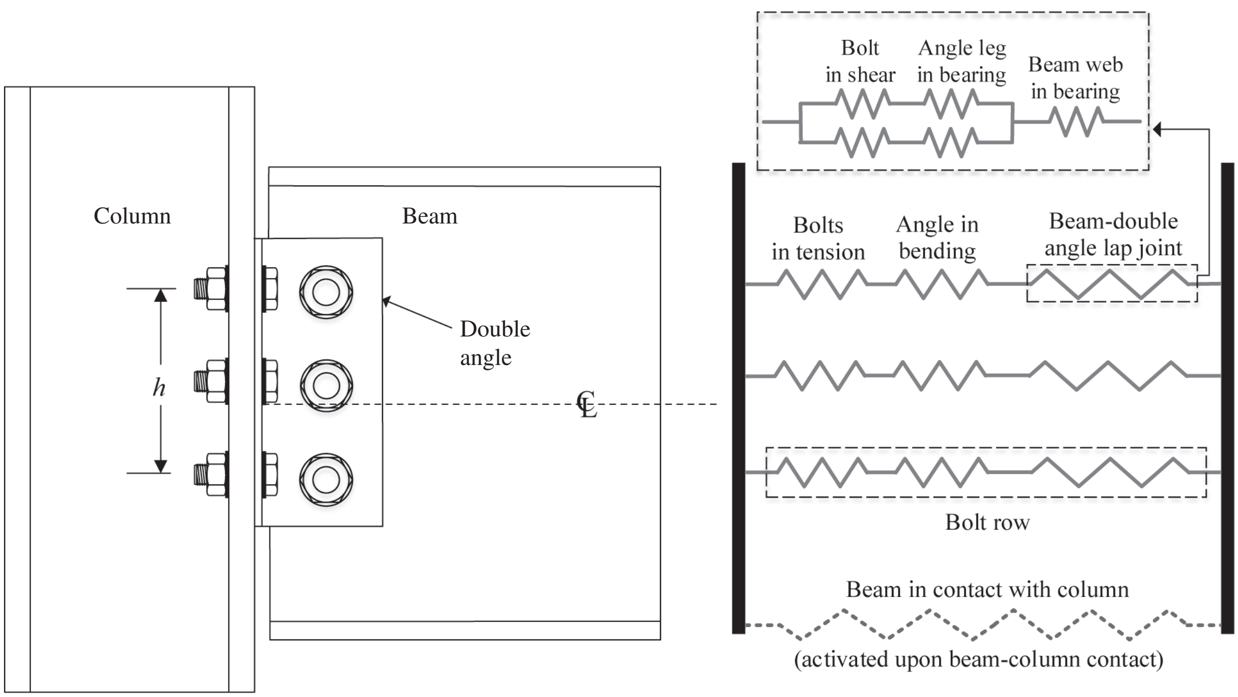

(b) Double-angle connection

Fig. 1. Connection configuration and stiffness model.

where M is the moment resulted from the shear and tension forces applied on the beam and is affected by the location of the center of rotation.

LIMIT STATES AND FAILURE MODES

The ultimate capacity of each spring component is incorporated in the stiffness model by identifying all limit states and failure modes in simple steel connections. The potential limit states of the shear tab and the double-angle connections are presented below.

Weld Strength

The weld available strength, R_{nw}, can be calculated using AISC *Specification* (2016) Section J2.4:

$$R_{nw} = 0.6F_{EXX}K_{wt}(1+0.5\sin^{1.5}\theta)A_{we} \tag{14}$$

where K_{wt} is the temperature-dependent retention factor for the strength of the weld material, F_{EXX} is the filler metal classification strength at ambient temperature, θ is the angle between the line of action of the required force and the weld longitudinal axis, and A_{we} is the effective area of the weld.

Bolt Slip Resistance

To represent the inherent friction strength between steel plates due to the normal force exerted by bolt tightening, the bolt slip resistance, R_s, is calculated using AISC *Specification* Section J3.8:

$$R_s = \mu D_u h_f T_b n \tag{15}$$

where μ is the mean slip coefficient, D_u is the ratio of the mean installed bolt pretension to the specified minimum bolt pretension, T_b is the minimum pretension force applied on the bolt, h_f is a factor of fillers, and n is the number of slip/shear planes.

Bolt Shear Strength

To determine the shear resistance per shear plane of a bolt, R_v, AISC *Specification* Section J3.6 is used:

$$R_v = 0.625K_{bt}F_{ub}A_b \tag{16}$$

Bolt Tensile Strength

To predict the tensile strength of a bolt, R_t, subjected to a combined tensile and shear forces, the following equation is used from AISC *Specification* Section J3.6:

$$R_t = 0.83K_{bt}F_{ub}A_b \tag{17}$$

Plate or Angle Leg Bearing and Tearout Resistance

To define the available strength of the plate or angle leg in bearing and tearout, R_{br}, the following equation is used from AISC *Specification* Section J3.10:

$$R_{br} = 3.0K_{ut}F_{ut}d_b t \leq 1.5l_c t K_{ut}F_{ut} \tag{18}$$

where l_c is the clear distance between the edge of the hole and the edge of the adjacent hole or edge of the material.

Punching Shear Resistance

The shear resistance of the plate against bolt punching, R_{pn}, can be determined using the following equation from Eurocode 3 (CEN, 2005b), Section 3.6:

$$R_{pn} = 0.6\pi d_m t K_{ut}F_{ut} \tag{19}$$

where d_m is the mean of the across points and across flats dimensions of the bolt head or the nut, whichever is smaller.

Shear Yielding of Plate or Angle Leg

The available shear strength for shear yielding of the element, R_{vy}, is determined using AISC *Specification* Section J4.2:

$$R_{vy} = 0.6K_{yt}F_{yt}A_s \tag{20}$$

where A_s is the gross area subject to shear.

Shear Rupture of Plate or Angle Leg

The available shear strength for shear rupture of the element, R_{vu}, is determined using AISC *Specification* Section J4.2:

$$R_{vu} = 0.6K_{ut}F_{ut}A_{s,net} \tag{21}$$

where $A_{s,net}$ is the net area subject to shear.

Block Shear Rupture of Plate or Angle Leg

The available strength for block shear of the plate, R_{bs}, can be calculated using AISC *Specification* Section J4.3:

$$R_{bs} = U_{bs}K_{ut}F_{ut}A_{nt} + \min\left\{\begin{matrix} 0.6K_{ut}F_{ut}A_{nv} \\ 0.6K_{yt}F_{yt}A_{gv} \end{matrix}\right\} \tag{22}$$

where U_{bs} is the tension stress distribution factor, A_{nt} is the net area subject to tension, A_{nv} is the net area subject to shear, and A_{gv} is the gross area subject to shear.

Angle Leg in Bending

The bending behavior of the bolted connections is similar to that of the T-stub during tension. Consequently, the capacity of the angle leg in bending is similar to that of an equivalent T-stub in tension. Therefore, the bending capacity of the angle leg, R_b, for each bolt-row is represented by the following equation from Eurocode 3, Section 6.2.4:

$$R_b = \frac{4M_p}{m} \tag{23}$$

where M_p is the plastic moment capacity and can be calculated using the following equation:

$$M_p = 0.25 l_{eff,ab} t^2 K_{yt} F_{yt} \tag{24}$$

Flexural Yielding of Plate or Angle Leg

The available flexural strength in flexural yielding of the plate and the web angle leg, M_y, is determined using AISC *Specification* Section J.4.5:

$$M_y = K_{yt} F_{yt} Z_x \tag{25}$$

where Z_x is the plastic section modulus of the plate or angle leg.

Flexural Rupture of Plate or Angle Leg

The available flexural strength in flexural rupture, M_u, of the plate and the web angle leg is determined using AISC *Specification* Section J.4.5:

$$M_u = K_{ut} F_{ut} Z_{net} \tag{26}$$

where Z_{net} is the net plastic section modulus of the plate or angle leg.

BEHAVIOR OF SIMPLE CONNECTIONS IN FIRE

In this section, the general behavior of simple connections (shear tab and double angle) is divided into several phases shown in Figure 2. The phases are as follows:

Phase 1: Pre-Slip

During the initial phase, the bolts are pretensioned and the loading is applied. The response of the connection at this phase is linear and has a relatively high stiffness until the forces applied on the bolts reach the value of the slip-resistance force (Equation 15).

Phase 2: Slip

During the slip phase, the applied force on the bolts reached the bolt-slip resistance force, and slippage of the shear bolts starts having a value of $s_{slip} = d_h - d_b$ where s_{slip} is the horizontal distance that allows the bolt to slip freely before having contact with the edge of the bolt hole, and d_h is the diameter of the bolt hole. The angle at which the bolt is in contact with the bolt hole, $\theta_{bolt\text{-}contact}$, can be calculated using the following equation:

$$\theta_{bolt\text{-}contact} = \frac{s_{slip}}{p}\left(\frac{180}{\pi}\right) \tag{27}$$

where p is the vertical distance between the center of rotation and the farthest bolt-row of the connection.

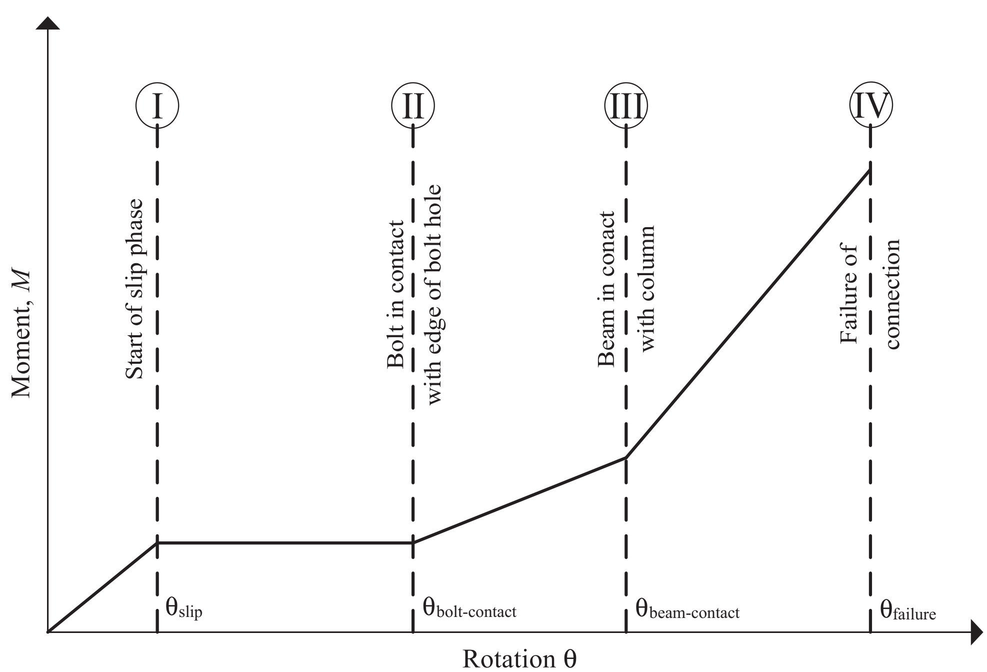

Fig. 2. Idealized behavior of shear tab and double-angle connections.

Phase 3: Bolt Contact

During this phase, the top and bottom bolts are in contact with the bolt holes, and the stiffness of the connection decreases gradually up to a degree of rotation where the contact occurs between the beam and the column flange. The angle at which the contact occurs between the beam and column can be calculated by the following equation:

$$\theta_{beam\text{-}contact} = \frac{s + s_{slip}}{D}\left(\frac{180}{\pi}\right) \tag{28}$$

where s is the setback distance between the beam and the column, and D is the distance between the beam bottom flange and the center of rotation of the connection before contact.

Phase 4: Beam Contact

Once the beam is in contact with the column, the stiffness of the connection increases and the center of rotation shifts from the middle bolt to the contact between the beam flange and the column. Moreover, the major differences in the behavior of the connection before and after beam-column contact are illustrated in Figure 3.

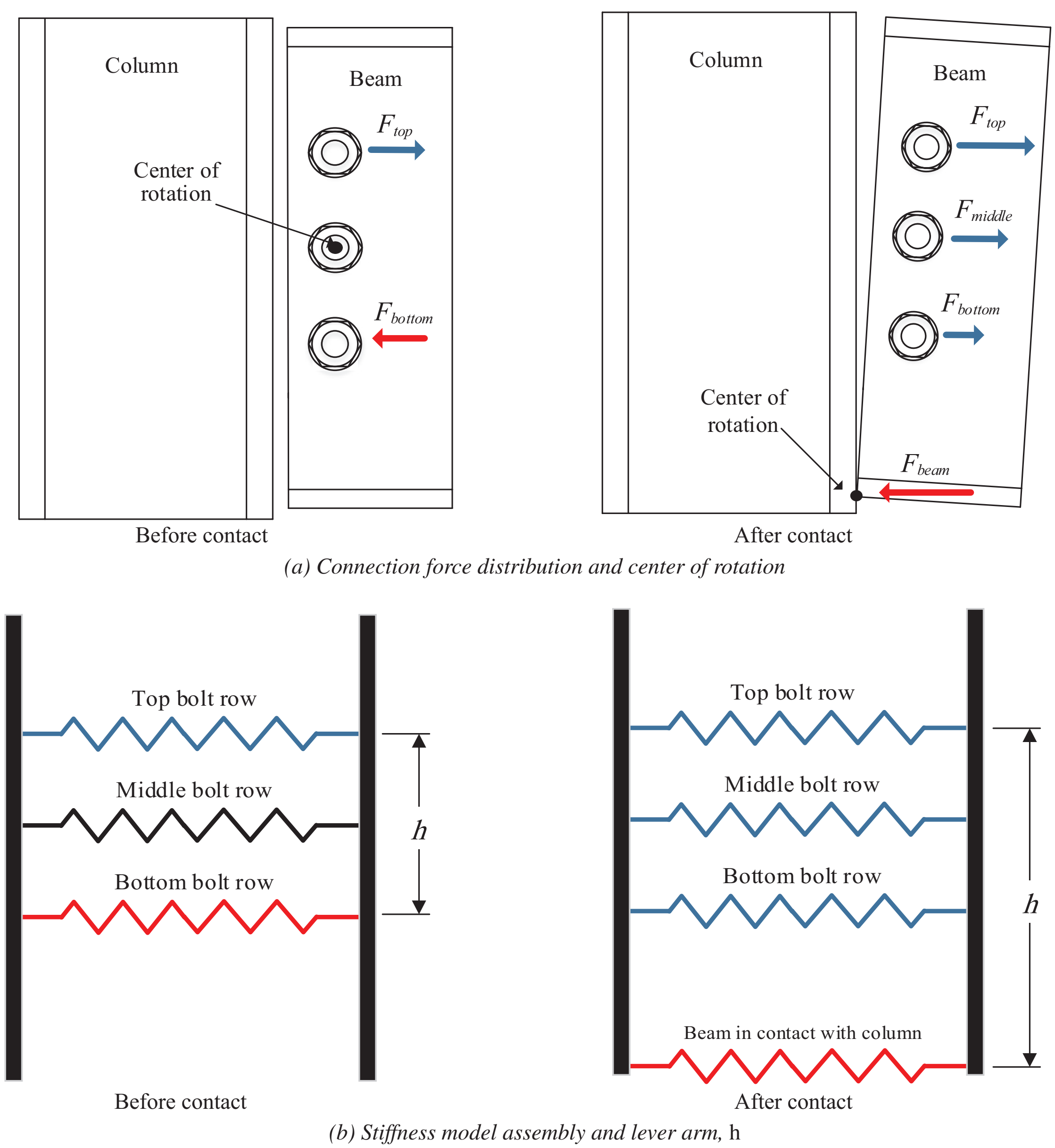

Fig. 3. Simple connections response before and after beam-column contact.

Table 1. Failure Modes of Simple Connections at Different Temperatures (Experiment vs. Stiffness Model)									
Type of Connection	Temperature		Failure Mode		Capacity				% Error
					Experiment		Stiffness Model		
	°C	°F	Experiment	Stiffness Model	kN	kips	kN	kips	
Double angle	20	68	Bolt punching the angle leg followed by block shear	Bolt punching the angle leg	243	54.6	179	40.2	26.3
	450	842	Flexural rupture of angle leg	Flexural rupture of angle leg	113	25.4	108	24.3	4.4
	550	1020	Flexural rupture of angle leg	Flexural rupture of angle leg	59.7	13.4	57.5	12.9	3.7
	650	1200	Shear bolt failure	Shear bolt failure	31.6	7.10	39.6	8.90	25.3
Shear tab	20	68	Shear bolt failure	Shear bolt failure	185	41.6	142	31.9	23.2
	450	842	Shear bolt failure	Shear bolt failure	84.0	18.9	72.3	16.3	13.9
	550	1020	Shear bolt failure	Shear bolt failure	38.5	8.66	42.9	9.64	11.4
	650	1200	Shear bolt failure	Shear bolt failure	19.3	4.34	19.1	4.29	1.04

Incremental Technique

The load-rotation response of the connections is predicted using an incremental analysis technique. The connection rotation is computed at an increment of 1.5 kN (0.34 kip) from the total applied force; thus force control is used in the analysis. The increment size is chosen to be small in order to obtain accurate results specifically when the center of rotation shifts from the middle of the shear bolts to the center of the bottom flange (contact phases). In this case, the lever arm h increases, and consequently the bolt forces are redistributed as shown in Figure 3. The connection is considered to fail when one of the connection components reaches its maximum capacity. Note that the tangent modulus is used in the components' material properties to account for material yielding.

Comparing Results

The two sets of experiments performed at the University of Sheffield (Yu et al., 2009a, 2009c) are used to examine the ability of the proposed model to predict the behavior of the shear tab and the double-angle connections. The details of the connections used in the experiment are shown in Figures 4(a) and 4(b). Figures 5(a) and 5(b) show that the proposed stiffness models are in good agreement with the experimental results of shear tab and double-angle connections, respectively, at ambient and elevated temperatures. Furthermore, the stiffness models are able to predict the ultimate strength, failure modes, and rotational capacities of the isolated simple connections.

Table 1 summarizes the comparison of failure capacities observed in the experiments and predicted using the stiffness model for each connection at ambient and elevated temperatures. It can be seen that the stiffness model can predict the failure modes and capacities when compared with experimental tests performed at elevated temperatures on the shear tab and double-angle connections (University of Sheffield, 2007).

Limitations and Assumptions of the Proposed Stiffness Model

- The excessive ovalization of the shear bolt holes was not taken into consideration in the proposed model, which underpredicts the full strength and ductility of the shear tab and the double-angle connections at ambient temperature as shown in Figures 5(a) and 5(b) and Table 1.
- The proposed stiffness model is able to predict the behavior of the simple connections up to the first component failure. The following fracture mechanism was not included in the proposed model. However, failure was predicted as the steel material reaches its ultimate strength.
- The stiffness model is developed for fast heating cases, thus the time-dependent properties of steel (thermal creep effect) are not considered.

FIRE DESIGN EXAMPLES OF SIMPLE CONNECTIONS

A step-by-step procedure that incorporates the developed stiffness model in the fire design of steel connections is presented. The procedure is thoroughly explained in the two examples: shear tab and double-angle connections in an isolated frame. Some assumptions are made to propose a simple and conservative fire design guideline. The examples

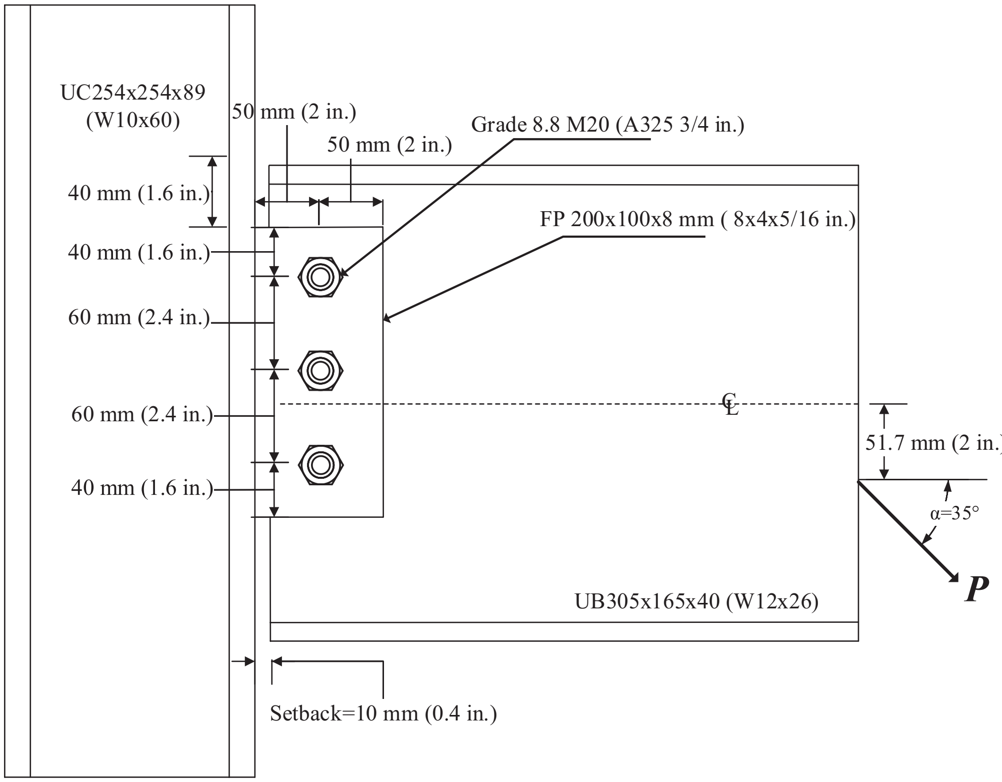

(a) Shear tab connection

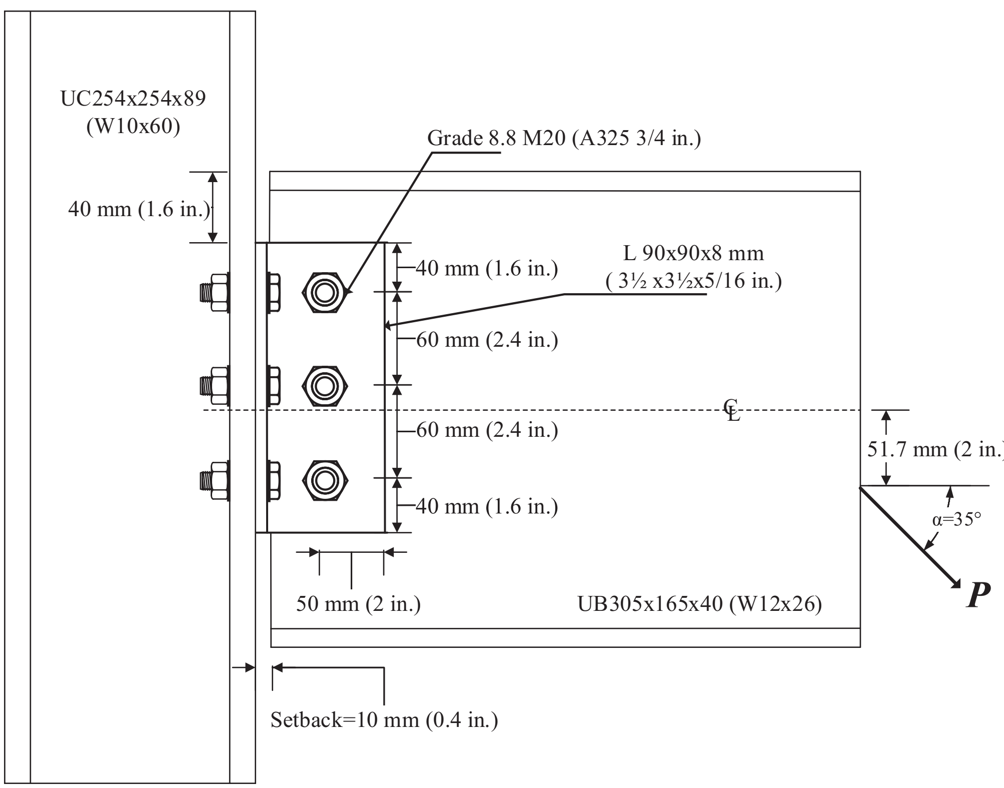

(b) Double-angle connection

Fig. 4. Details of the isolated connections (University of Sheffield, 2007).

illustrate the different key aspects in designing both shear tab and double-angle connections when subjected to fire. Afterward, a comparison between the two connections' design is duly made based on the results and conclusions are drawn.

Design Criteria

The primary goal of the presented study, which is illustrated in the following two examples, is to design the shear connection to maintain the load transfer between the beam and the column at least before the failure of the steel beam in fire events. The beam failure in most cases resembles the beam catenary action initiation (formation of plastic hinges), which occurs at very high fire temperatures. Consequently, and due to excessive beam sagging, tensile forces are exerted on the connections, causing them to fail. However, the study focuses on designing the connection to maintain the load transfer as long as the beam remains intact. This will prevent or at least delay the failure of the system; allowing more time for occupants to evacuate the building.

Three factors need to be taken into consideration when designing simple steel connections under fire conditions: gravity loads, induced axial load due to thermal expansion, and moment demand exerted by the beam on the connection. It is worth mentioning that transient-state conditions of fire are considered. The temperature is increased from ambient temperature, 20°C (68°F), up to the target temperature. The slip of shear planes is implicitly included in the stiffness model. The connection and the beam are uniformly heated.

In many fire tests, the columns were observed to remain in the elastic region during fire. As the primary structural

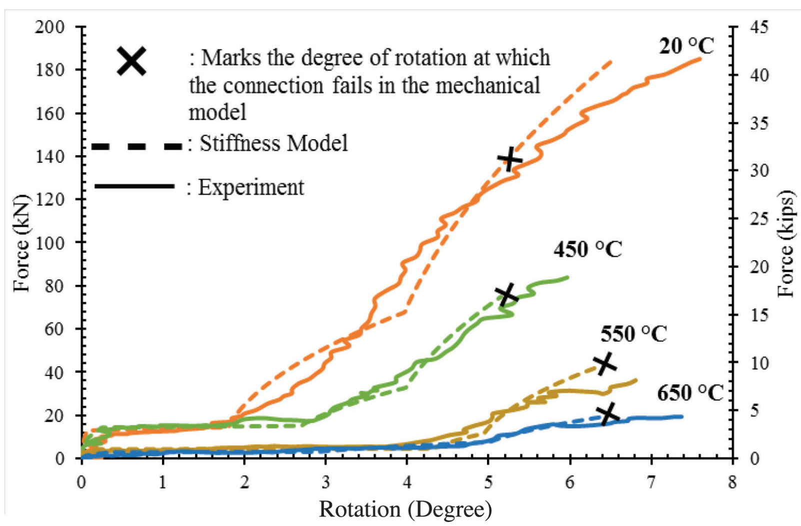

(a) Shear tab connection

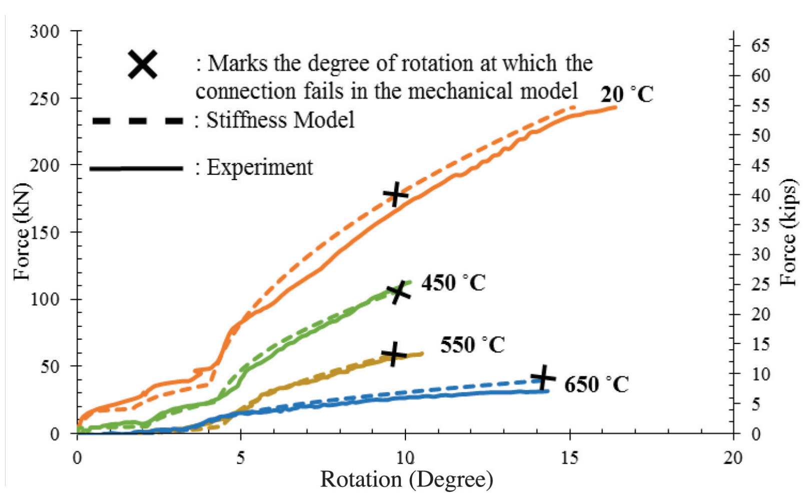

(b) Double-angle connection

Fig. 5. Comparison between results from experiments and stiffness model.

Table 2. Material Properties Retention Factors at Different Temperatures						
		Temperature (°C)				
Retention Factor	Reference	20	400	500	600	700
Modulus of elasticity, K_E	Lee et al. (2013)	1.0	0.89	0.77	0.57	0.26
Base material yield strength, K_{yt}	Lee et al. (2013)	1.0	0.72	0.66	0.44	0.21
Base material ultimate strength, K_{ut}	Lee et al. (2013)	1.0	0.97	0.64	0.37	0.18
Bolt ultimate strength, K_{bt}	Hu et al. (2007)	1.0	0.66	0.379	0.19	0.06
Weld ultimate strength, K_{wt}	Eurocode 3 (CEN, 2005a)	1.0	0.876	0.627	0.378	0.13

element in steel structures, columns are usually protected using insulating material to reduce the column temperature increase during fire. Thus, the columns are assumed to be insulated, and the column temperature can be roughly estimated to reach 60% of the (unprotected) beam temperature as shown in previous studies (Zhang and Usmani, 2015). Columns are assumed to be fixed from both ends against rotation and translation. The frame is perfectly symmetrical in loading and geometry.

Design Steps

First, the connection is designed to meet both serviceability and strength requirements prescribed in the structural design codes at ambient temperature and under gravity loads only. The applied loads, due to fire, are calculated, and the stresses on each component of the connection are obtained. These additional stresses are the induced axial forces due to the restrained thermal expansion and the moment demand on the connection due to beam sagging and rotation. It is well known that the column stiffness is the controlling factor in determining the magnitude of the induced axial force in the beam by providing the beam end axial restraint (Wang et al., 2011). Therefore, when calculating the thermal induced axial forces, only the column flexural stiffness is considered for simplicity. This assumption is valid and considered conservative because the beam axial stiffness is relatively high when compared with the column flexural stiffness. The induced axial force is calculated first by quantifying the change of the beam length due to thermal expansion and including it as an imposed horizontal deflection at the midspan of the column. Then, by knowing the column stiffness, the induced axial force can be easily calculated.

The moment applied on the connection is obtained by a simple graphical solution, where the beam end rotational stiffness (beam-line) and the connection rotational stiffness (based on the developed stiffness model) are plotted and the moment demand (intersection between the two curves) is obtained. After obtaining the new stresses, all the connection limit states are checked, while multiplying each equation by its corresponding retention factor. These retention factors are in function of temperature and they are summarized in Table 2. The connection is redesigned accordingly. These steps are repeated until reaching a final connection configuration that can withstand the additional stresses while considering strength degradation.

DESIGN EXAMPLE 1— SINGLE-PLATE SHEAR CONNECTION IN FIRE

Given:

Check the single-plate shear connection shown in Figure 6 when subjected to fire conditions. The beam is an ASTM A992 W16×40 with a length of L = 20 ft. The column is an ASTM A992 W10×49 with a height of H = 20 ft. The column is assumed to be fixed at both ends with a floor height of 10 ft. The beam and connection are unprotected; the column is protected.

The beam is connected to the column using an ASTM A572 Grade 50 single plate with one column of three ¾-in.-diameter Group A bolts. The threads are not included in the shear plane (thread condition X). The beam setback is 0.4 in.

The beam and the connection are uniformly heated from an ambient temperature of 20°C (68°F) up to 500°C (932°F). The beam is assumed to carry a maximum of half its plastic moment strength at ambient temperature. The beam top flange is laterally supported along its length. Thermal creep effect is not included.

Solution:

From AISC *Manual* (2017) Tables 2-4 and 2-5, the material properties are as follows:

Beam and column
ASTM A992
$F_y = 50$ ksi
$F_u = 65$ ksi

Plate
ASTM 572, Grade 50
$F_y = 50$ ksi
$F_u = 65$ ksi

From AISC *Manual* Table 1-1, the geometric properties are as follows:

Beam
W16×40
$d = 16.0$ in.
$t_w = 0.305$ in.
$S_x = 64.7$ in.^{3}
$Z_x = 73.0$ in.^{4}

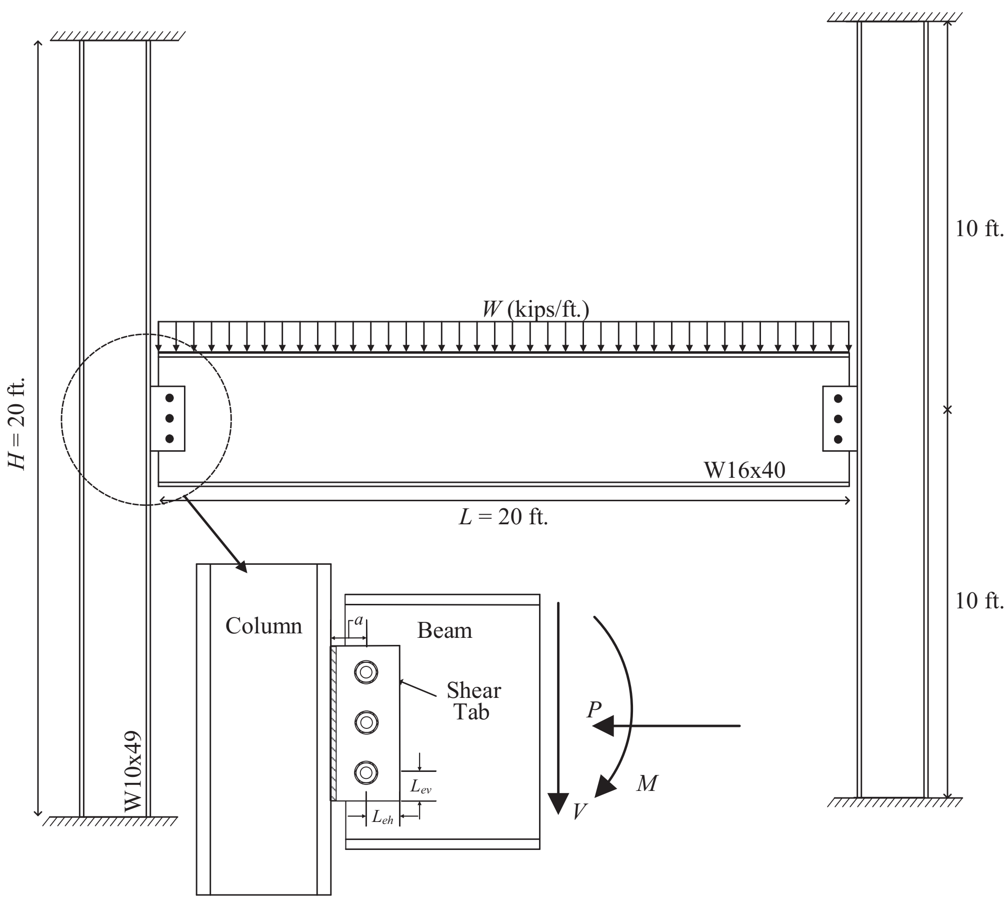

Fig. 6. Example 1 configuration of column-beam frame system connected with a single plate.

Column
W10×49
$I_x = 272 \text{ in.}^4$

From Table 2, the material property retention factors at 500°C (932°F) are:

$K_E = 0.77$
$K_{yt} = 0.66$
$K_{ut} = 0.64$
$K_{bt} = 0.379$
$K_{wt} = 0.627$

Step 1—Compute the Applied Distributed Load

The maximum moment developed at mid-span of the beam is determined using AISC *Manual* Table 3-23, Case 1:

$$M_{max} = \frac{wL^2}{8}$$

The beam plastic moment is determined from AISC *Specification* Equation F2-1:

$$M_p = Z_x F_y \qquad (\textit{Spec}.\text{ Eq. F2-1})$$
$$= \frac{(73.0 \text{ in.}^3)(50 \text{ ksi})}{12 \text{ in./ft}}$$
$$= 304 \text{ kip-ft}$$

The applied load should exert a maximum moment of 50% of the beam plastic moment capacity at ambient temperature; therefore:

$$w = \frac{8(0.5M_p)}{L^2}$$
$$= \frac{8(0.5)(304 \text{ kip-ft})}{(20 \text{ ft})^2}$$
$$= 3.04 \text{ kip/ft}$$

Use $w = 3$ kip/ft

Step 2—Single-Plate Shear Connection Configuration

The single-plate shear connection is designed following the AISC *Manual* Part 10, Single-Plate Shear Connections—Conventional Configuration. Try a ⅜-in.-thick plate with $l_{ev} = 1\frac{1}{2}$ in., $l_{eh} = 2$ in. and $s = 2\frac{1}{2}$ in.

From AISC *Specification* Table J3.4, the minimum vertical edge distance, for a ¾-in.-diameter bolt is 1 in.:

$l_{ev} = 1\frac{1}{2} \text{ in.} > 1 \text{ in.}$ **o.k.**

From AISC *Manual* Part 10, the minimum horizontal edge distance is: $2d = 2(\frac{3}{4} \text{ in.}) = 1\frac{1}{2}$ in.

$l_{ev} = 2 \text{ in.} > 1\frac{1}{2} \text{ in.}$ **o.k.**

The maximum plate thickness is determined using AISC *Manual* Table 10-9. For three bolts in STD holes:

$$t_{p,max} = \frac{d}{2} + \frac{1}{16} \text{ in.}$$
$$= \frac{\frac{3}{4} \text{ in.}}{2} + \frac{1}{16} \text{ in.}$$
$$= 0.438 \text{ in.} > \frac{3}{8} \text{ in.} \quad \textbf{o.k.}$$

With a setback distance equal to 0.4 in., use $a = 2\frac{1}{2}$ in. From AISC *Manual* Table 10-9, with three bolts in STD holes, the eccentricity is:

$$
\begin{aligned}
e &= \frac{a}{2} \\
&= \frac{2\frac{1}{2}\text{ in.}}{2} \\
&= 1.25\text{ in.}
\end{aligned}
$$

The minimum length of the plate should be greater than half the depth of the beam. The minimum bolt spacing is determined as follows:

$$
\begin{aligned}
s &= \left(\frac{1}{n-1}\right)\left(\frac{d}{2} - 2l_{ev}\right) \\
&= \left(\frac{1}{3-1}\right)\left[\frac{16.0\text{ in.}}{2} - 2(1\frac{1}{2}\text{ in.})\right] \\
&= 2\frac{1}{2}\text{ in.}
\end{aligned}
$$

From AISC *Manual* Part 10, the required fillet weld size for a ⅜-in.-thick plate is:

$$
\begin{aligned}
\tfrac{5}{8}t_p &= (\tfrac{5}{8})(\tfrac{3}{8}\text{ in.}) \\
&= 0.234\text{ in.}
\end{aligned}
$$

Use ¼-in. fillet welds.

Step 3—Check the Beam Strength

Step 3a—Check for beam catenary action

The maximum moment in the beam (at mid-span) is determined using AISC *Manual* Table 3-23, Case 1:

$$
\begin{aligned}
\frac{wL^2}{8} &= \frac{(3\text{ kip/ft})(20\text{ ft})^2}{8} \\
&= 150\text{ kip-ft}
\end{aligned}
$$

The beam elastic moment capacity is:

$$
\begin{aligned}
K_{yt}F_{yt}S_x &= \frac{0.66(50\text{ ksi})(64.7\text{ in.}^3)}{12\text{ in./ft}} \\
&= 178\text{ kip-ft} > 150\text{ kip-ft}
\end{aligned}
$$

The beam will remain in the elastic zone; no catenary action will occur.

Step 3b—Check beam shear strength

The maximum shear applied on the beam (at the support) is determend using AISC *Manual* Table 3-23, Case 1:

$$
\begin{aligned}
V &= \frac{wL}{2} \\
&= \frac{(3\text{ kip/ft})(20\text{ ft})}{2} \\
&= 30.0\text{ kips}
\end{aligned}
$$

The shear yielding strength of the beam is determined as follows:

$$\begin{aligned} A_s &= dt_w \\ &= (16.0 \text{ in.})(0.305 \text{ in.}) \\ &= 4.88 \text{ in.}^2 \end{aligned}$$

$$\begin{aligned} 0.6K_{yt}F_{yt}A_s &= 0.6(0.66)(50 \text{ ksi})(4.88 \text{ in.}^2) \\ &= 96.6 \text{ kips} > 30.0 \text{ kips} \quad \textbf{o.k.} \end{aligned}$$

Step 4—Determine the Forces on the Connection

Step 4a—Shear force on the connection due to gravity load

The shear force at the connection is determend using AISC *Manual* Table 3-23, Case 1:

$$\begin{aligned} V &= \frac{wL}{2} \\ &= \frac{(3 \text{ kip/ft})(20 \text{ ft})}{2} \\ &= 30.0 \text{ kips} \end{aligned}$$

Step 4b—Compressive force on the connection due to thermal expansion of the beam

The coefficient of thermal expansion coefficient is:

$$\begin{aligned} \alpha &= 1.2(10^{-5})/{}^\circ\text{C} \\ &= 6.67(10^{-6})/{}^\circ\text{F} \end{aligned}$$

The elongation of the beam due to thermal expansion is:

$$\begin{aligned} \Delta l &= L(\Delta T)(\alpha) \\ &= (20 \text{ ft})(932^\circ\text{F} - 68^\circ\text{F})(6.67/{}^\circ\text{F})(10^{-6})(12 \text{ in./ft}) \\ &= 1.38 \text{ in.} \end{aligned}$$

Because the frame is symmetrical, the horizontal displacement at the column mid-span is:

$$\begin{aligned} \Delta &= \frac{\Delta l}{2} \\ &= \frac{1.38 \text{ in.}}{2} \\ &= 0.690 \text{ in.} \end{aligned}$$

The column temperature is roughly estimated to be 300°C (572°F), which is 60% of the beam temperature. From Table 3, the K_E at 300°C (572°F) is estimated at 0.90. Thus, the thermal compressive force applied to the connection is:

$$\Delta = \frac{PH^3}{48K_EEI_x}$$

Solving for P:

$$P = \frac{48\Delta K_E E I_x}{H^3}$$

$$= \frac{48(0.690\text{ in.})(0.90)(29{,}000\text{ ksi})(272\text{ in.}^4)}{(20\text{ ft})^3(12\text{ in/ft})^3}$$

$$= 17.0\text{ kips}$$

Step 4c—Moment applied at the connection

At ambient temperatures, designers consider the shear tab connection an ideally pinned connection where its moment demand is negligible. However, as temperature increases, the flexural stiffness of the connected beam decreases, and thus an increase in the connection rotation can be observed. Due to this excessive rotation, the bending moment applied on the shear plate cannot be ignored, and it is important to take it into consideration in fire design. A simple way to calculate the applied moment is by getting the intersection between the beam line (also called load line) and the connection stiffness by which the moment and end rotation are obtained. The beam line is a straight line that can be plotted from the moment and end rotation for a fixed-end beam and simply supported beam.

For a simply supported beam:

$$\theta_c = \frac{wL^3}{24 K_E E I_x}$$

$$= \frac{(3\text{ kip/ft})(20\text{ ft})^3(12\text{ in./ft})^2}{24(0.771)(29{,}000\text{ ksi})(518\text{ in.}^4)}$$

$$= 0.0124\text{ rad}$$

$$M = 0\text{ kip-in.}$$

For a fixed-end beam:

$$\theta_c = 0\text{ rad}$$

$$M = \frac{wL^2}{12}$$

$$= \frac{(3\text{ kip/ft})(20\text{ ft})^2(12\text{ in./ft})}{12}$$

$$= 1{,}220\text{ kip-in.}$$

The beam-line and moment-rotation characteristics (using stiffness model) of the connection are plotted in Figure 7. The moment applied to the connection is determined at the intersection of these two lines. Use M = 17.7 kip-in.

M is used to check the strength of the shear tab connection when subjected to beam-end moments.

Step 5—Compute the Applied Shear Force on the Bolts

Step 5a—Bolt shear force due to gravity load

$$V_v = \frac{V}{n}$$

$$= \frac{30.0\text{ kips}}{3\text{ bolts}}$$

$$= 10.0\text{ kips/bolt}$$

Step 5b—Bolt shear force due to thermal expansion

$$V_p = \frac{P}{n}$$
$$= \frac{17.0 \text{ kips}}{3 \text{ bolts}}$$
$$= 5.67 \text{ kips/bolt}$$

Step 5c—Bolt shear force due to the applied moment on the connection

$$V_m = \frac{M}{(n-1)s}$$
$$= \frac{17.7 \text{ kip-in.}}{(3-1)(2\tfrac{1}{2} \text{ in.})}$$
$$= 3.54 \text{ kips/bolt}$$

Step 5d—Applied shear force on each bolt

$$V_{top} = \sqrt{(V_m - V_p)^2 + (V_v)^2}$$
$$= \sqrt{(3.54 \text{ kips} - 5.67 \text{ kips})^2 + (10.0 \text{ kips})^2}$$
$$= 10.2 \text{ kips}$$

$$V_{middle} = \sqrt{(V_p)^2 + (V_v)^2}$$
$$= \sqrt{(5.67 \text{ kips})^2 + (10.0 \text{ kips})^2}$$
$$= 11.5 \text{ kips}$$

$$V_{bottom} = \sqrt{(V_p + V_m)^2 + (V_v)^2}$$
$$= \sqrt{(3.54 \text{ kips} + 5.67 \text{ kips})^2 + (10.0 \text{ kips})^2}$$
$$= 13.6 \text{ kips}$$

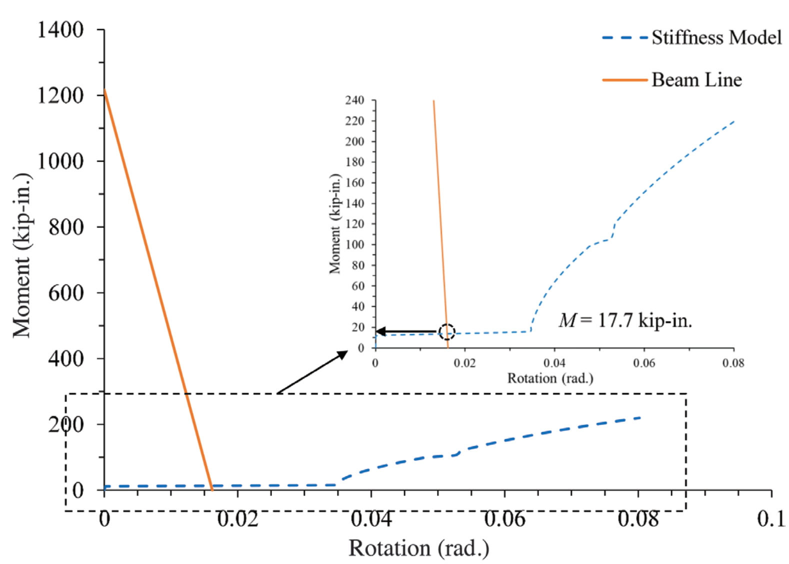

Fig. 7. Moment demand on the shear tab connection using beam-line theory.

Step 6—Determine the Strength of the Plate

Step 6a—Shear yielding

$$A_s = lt_p$$
$$= (8.00 \text{ in.})(3/8 \text{ in.})$$
$$= 3.00 \text{ in.}^2$$

$$R_{vy} = 0.6K_{yt}F_{yt}A_s$$
$$= 0.6(0.66)(50 \text{ ksi})(3.00 \text{ in.}^2)$$
$$= 59.4 \text{ kips} > 30.0 \text{ kips} \quad \textbf{o.k.}$$

Step 6b—Shear rupture

$$A_n = \left[l - n\left(d + 1/16 \text{ in.}\right)\right]t_p$$
$$= \left[8.00 \text{ in.} - 3(13/16 \text{ in.} + 1/16 \text{ in.})\right](3/8 \text{ in.})$$
$$= 2.02 \text{ in.}^2$$

$$R_{vu} = 0.6K_{ut}F_{ut}A_n$$
$$= 0.6(0.64)(65 \text{ ksi})(2.02 \text{ in.}^2)$$
$$= 50.4 \text{ kips} > 30.0 \text{ kips} \quad \textbf{o.k.}$$

Step 6c—Flexural yielding

$$Z_x = \frac{t_p l^2}{4}$$
$$= \frac{(3/8 \text{ in.})(8.00 \text{ in.})^2}{4}$$
$$= 6.00 \text{ in.}^3$$

$$M_y = K_{yt}F_{yt}Z_x$$
$$= 0.66(50 \text{ ksi})(6.00 \text{ in.}^3)$$
$$= 198 \text{ kip-in.} > 17.7 \text{ kip-in.} \quad \textbf{o.k.}$$

Step 6d—Flexural rupture

The net plastic section modulus is not calculated here. Use $Z_{net} = 3.56 \text{ in.}^3$

$$M_u = K_{ut}F_{ut}Z_{net}$$
$$= 0.64(65 \text{ ksi})(3.56 \text{ in.}^3)$$
$$= 148 \text{ kip-in.} > 17.7 \text{ kip-in.} \quad \textbf{o.k.}$$

Step 6e—Block shear rupture

$$R_n = 0.60A_{nv}K_{ut}F_{ut} + U_{bs}A_{nt}K_{ut}F_{ut} \leq 0.60A_{gv}K_{yt}F_{yt} + U_{bs}A_{nt}K_{ut}F_{ut}$$

where

$$A_{nt} = \left[2.00 \text{ in.} - 0.5(13/16 \text{ in.} + 1/16 \text{ in.})\right](3/8 \text{ in.})$$
$$= 0.586 \text{ in.}^2$$

$$A_{gv} = (5.00 \text{ in.} + 1\tfrac{1}{2} \text{ in.})(\tfrac{3}{8} \text{ in.})$$
$$= 2.44 \text{ in.}^2$$

$$A_{nv} = \left[(5.00 \text{ in.} + 1\tfrac{1}{2} \text{ in.}) - 2.5(\tfrac{13}{16} \text{ in.} + \tfrac{1}{16} \text{ in.})\right](\tfrac{3}{8} \text{ in.})$$
$$= 1.62 \text{ in.}^2$$

$$U_{bs} = 1.0$$

$$0.60 A_{nv} K_{ut} F_{ut} = 0.60(1.62 \text{ in.}^2)(0.64)(65 \text{ ksi})$$
$$= 40.4 \text{ kips}$$

$$0.60 A_{gv} K_{yt} F_{yt} = 0.60(2.44 \text{ in.}^2)(0.66)(50 \text{ ksi})$$
$$= 48.3 \text{ kips}$$

$$U_{bs} A_{nt} K_{ut} F_{ut} = 1.0(0.586 \text{ in.}^2)(0.64)(65 \text{ ksi})$$
$$= 24.4 \text{ kips}$$

$$R_n = 0.60 A_{nv} K_{ut} F_{ut} + U_{bs} A_{nt} K_{ut} F_{ut} \le 0.60 A_{gv} K_{yt} F_{yt} + U_{bs} A_{nt} K_{ut} F_{ut}$$
$$= 40.4 \text{ kips} + 24.4 \text{ kips} < 48.3 \text{ kips} + 24.4 \text{ kips}$$
$$= 64.8 \text{ kips} > 30.0 \text{ kips} \quad \textbf{o.k.}$$

Step 7—Weld Strength

$$f_v = \frac{V}{2l}$$
$$= \frac{30.0 \text{ kips}}{2(8.00 \text{ in.})}$$
$$= 1.88 \text{ kip/in.}$$

The moment applied to the weld is:

$$M + Ve = 17.7 \text{ kip-in.} + (30 \text{ kips})(1.25 \text{ in.})$$
$$= 55.2 \text{ kip-in.}$$

Maximum stress perpendicular to the weld is:

$$f_t = \frac{(M + Ve)\,l}{4(I_{weld})}$$
$$= \frac{12(55.2 \text{ kip-in.})(8.00 \text{ in.})}{4(8.00 \text{ in.})^3}$$
$$= 2.59 \text{ kip/in.}$$

Therefore, the maximum resultant force is:

$$\sqrt{f_t^2 + f_v^2} = \sqrt{(2.59 \text{ kips/in.})^2 + (1.88 \text{ kips/in.})^2}$$
$$= 3.20 \text{ kip/in.}$$

$$\theta = \tan^{-1}\left(\frac{f_t}{f_v}\right)$$
$$= \tan^{-1}\left(\frac{2.59 \text{ kips/in.}}{1.88 \text{ kips/in.}}\right)$$
$$= 54.0°$$

Table 3. Summary of the Limit State Avalable Strength of a Single-Plate Shear Connection in Fire [500°C (932°F)]	
Mode	**Available Strength**
Shear yielding of plate =	59.4 kips
Shear rupture of plate =	50.4 kips
Flexural yielding of plate =	198 kip-in.
Flexural rupture of plate =	148 kip-in.
Block shear of plate =	64.8 kips
Weld strength =	6.35 kip/in.
Bolt shear strength =	12.6 kips/bolt
Shear plate bearing and tearout strength =	24.8 kips/bolt
Beam bearing and tearout strength =	28.5 kips/bolt

$$
\begin{aligned}
R_{nw} &= 0.6K_{wt}F_{EXX}\left(1+0.5\sin^{1.5}\theta\right)A_{we} \\
&= 0.6(0.627)(70\text{ ksi})\left[1+0.5\sin^{1.5}(54.0°)\right](0.707)(\tfrac{1}{4}\text{ in.}) \\
&= 6.35\text{ kip/in.} > 3.20\text{ kip/in.}\quad \textbf{o.k.}
\end{aligned}
$$

Step 8—Check Shear Transfer at Bolts

Step 8a—Bolt shear strength

$$
\begin{aligned}
R_v &= 0.625nK_{bt}F_{ub}A_s \\
&= 0.625(1)(0.379)(120\text{ ksi})\left[\frac{\pi(\tfrac{3}{4}\text{ in.})^2}{4}\right] \\
&= 12.6\text{ kips/bolt}
\end{aligned}
$$

Step 8b—Plate bearing and tearout strength

$$
\begin{aligned}
R_{br} &= 3.0K_{ut}F_{ut}d_bt \le 1.5l_ctK_{ut}F_{ut} \\
&= 3.0(0.64)(65\text{ ksi})(\tfrac{3}{4}\text{ in.})(\tfrac{3}{8}\text{ in.}) \le 1.5(1.06\text{ in.})(\tfrac{3}{8}\text{ in.})(0.64)(65\text{ ksi}) \\
&= 24.8\text{ kips/bolt}
\end{aligned}
$$

Step 8c—Beam web bearing and tearout strength

$$
\begin{aligned}
R_{br} &= 3.0K_{ut}F_{ut}d_bt \le 1.5l_ctK_{ut}F_{ut} \\
&= 3.0(0.64)(65\text{ ksi})(\tfrac{3}{4}\text{ in.})(0.305\text{ in.}) \le 1.5(1.66\text{ in.})(0.305\text{ in.})(0.64)(65\text{ ksi}) \\
&= 28.5\text{ kips/bolt}
\end{aligned}
$$

Step 8d—Shear transfer at bolts

The shear transfer strength at the bolts is the minimum of the bolt shear strength, bearing and tearout strength at the plate, and bearing and tearout strength of the beam web.

$$
\begin{aligned}
R_v &= \min\{12.6\text{ kips/bolt, } 24.8\text{ kips/bolt, } 28.5\text{ kips/bolt}\} \\
&= 12.6\text{ kips/bolt}
\end{aligned}
$$

$$V_{top} = 10.2\text{ kips} < 12.6\text{ kips}\quad \textbf{o.k.}$$

$V_{middle} = 11.5 \text{ kips} < 12.6 \text{ kips}$ **o.k.**

$V_{bottom} = 13.6 \text{ kips} > 12.6 \text{ kips}$ **n.g.**

The connection will fail by shear rupture of the bottom bolt. Neglecting the thermal compressive forces, generated due to the expansion of the beam, and the moment demand leads to unsafe design. Increasing the bolt diameter or using a stronger bolt grade will produce a safe design.

A summary of the limit state capacities is presented in Table 3. The final design of the shear plate connection is shown Figure 8.

DESIGN EXAMPLE 2—DOUBLE-ANGLE CONNECTION IN FIRE

Given:

Check the double-angle shear connection shown in Figure 9 when subjected to fire conditions. The beam is an ASTM A992 W16×40 with a length of $L = 20$ ft. The column is an ASTM A992 W10×49 with a height of $H = 20$ ft. The column is assumed to be fixed at both ends with a floor height of 10 ft. The beam and connection are unprotected; the column is protected.

The beam is connected to the column using an ASTM A572 Grade 50 double angle. The beam is connected to the double angle through a single column of three bolts, and the double angle is connected to the column through two columns of three bolts. Bolts are ¾-in.-diameter Group A with the threads not included in the shear plane (thread condition X). The beam setback is 0.4 in.

The beam and the connection are uniformly heated from an ambient temperature of 20°C (68°F) up to 500°C (932°F). The beam is assumed to carry a maximum of half its plastic moment strength at ambient temperature. The beam top flange is laterally supported along its length. Thermal creep effect is not included.

Solution:

From AISC *Manual* Tables 2-4 and 2-5, the material properties are as follows:

Beam and column
ASTM A992
$F_y = 50$ ksi
$F_u = 65$ ksi

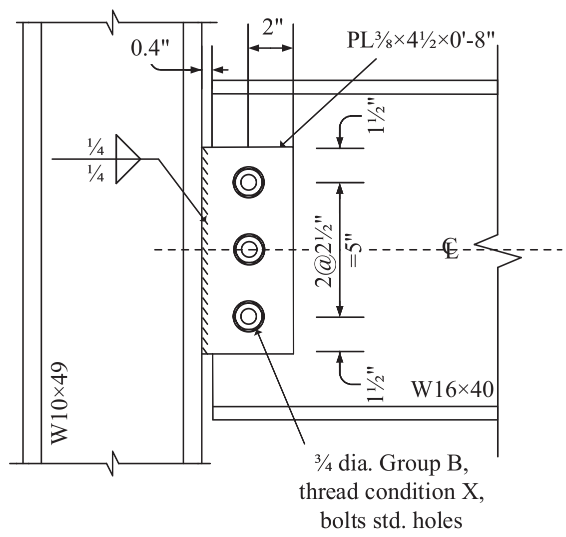

Fig. 8. Detailed design for W16×40 beam connected to W10×49 column through a single-plate connection.

Angle
ASTM 572, Grade 50
$F_y = 50$ ksi
$F_u = 65$ ksi

From AISC *Manual* Table 1-1, the geometric properties are as follows:

Beam
W16×40
$d = 16.0$ in.
$t_w = 0.305$ in.
$S_x = 64.7$ in.^{3}
$Z_x = 73.0$ in.^{3}

Column
W10×49
$I_x = 272$ in.^{4}

From Table 2, the material property retention factors at 500°C (932°F) are:

$K_E = 0.77$
$K_{yt} = 0.66$
$K_{ut} = 0.64$
$K_{bt} = 0.379$
$K_{wt} = 0.627$

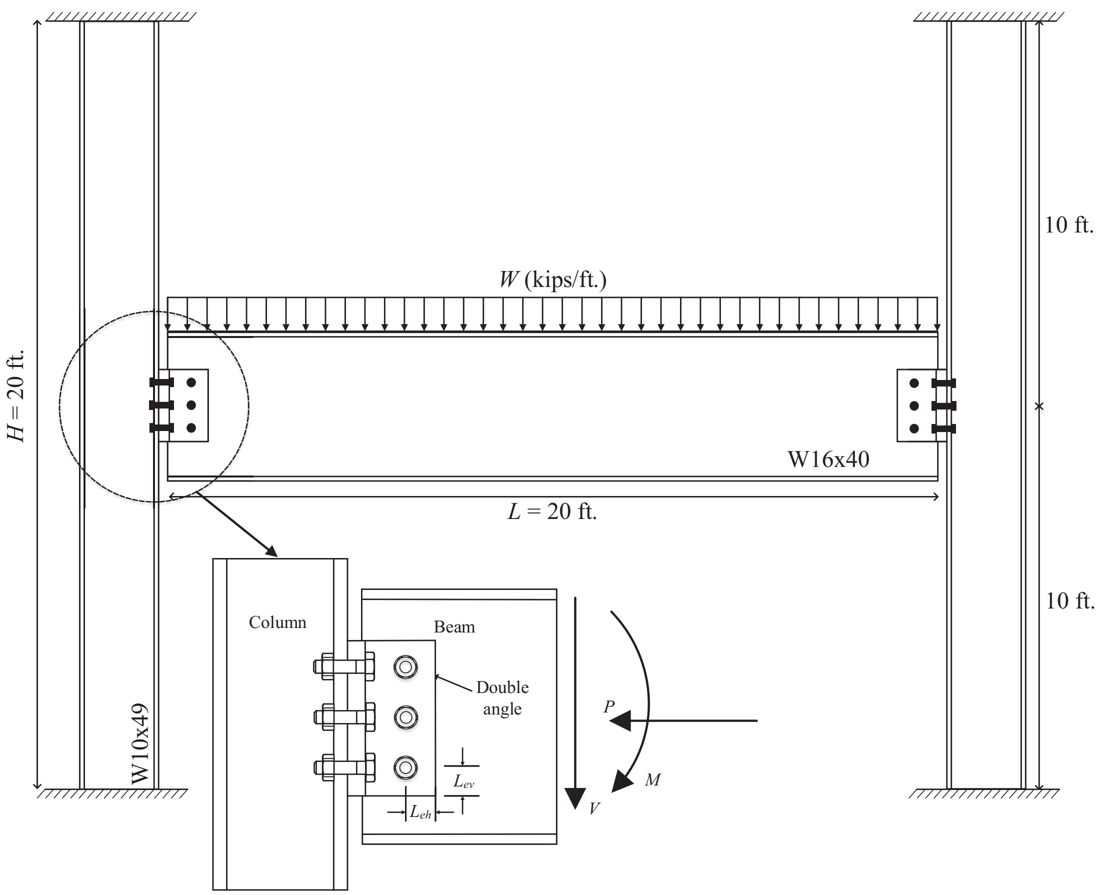

Fig. 9. Example 2 configuration of column-beam frame system connected with a double angle.

Step 1—Compute the Applied Distributed Load

The maximum moment developed at mid-span of the beam is determined using AISC *Manual* Table 3-23, Case 1:

$$M_{max} = \frac{wL^2}{8}$$

The beam plastic moment is determined from AISC *Specification* Equation F2-1:

$$\begin{aligned} M_p &= Z_x F_y \qquad \text{(}Spec\text{. Eq. F2-1)} \\ &= \frac{(73.0 \text{ in.}^3)(50 \text{ ksi})}{12 \text{ in./ft}} \\ &= 304 \text{ kip-ft} \end{aligned}$$

The applied load should exert a maximum moment of 50% of the beam plastic moment capacity at ambient temperature; therefore:

$$\begin{aligned} w &= \frac{8(0.5M_p)}{L^2} \\ &= \frac{8(0.5)(304 \text{ kip-ft})}{(20 \text{ ft})^2} \\ &= 3.04 \text{ kip/ft} \end{aligned}$$

Use $w = 3$ kip/ft

Step 2—Double-Angle Connection Configuration

Try L5×3½×⅜ angles with $l_{ev} = 1½$ in., $l_{eh} = 1½$ in. and $s = 2½$ in.

From AISC *Specification* Table J3.4, the minimum edge distance, for a ¾-in.-diameter bolts is 1 in.:

$$l_{ev} = 1\tfrac{1}{2} \text{ in.} > 1 \text{ in.} \quad \textbf{o.k.}$$

The minimum length of the angles should be greater than half the depth of the beam. The minumum bolt spacing is determined as follows:

$$\begin{aligned} s &= \left(\frac{1}{n-1}\right)\left(\frac{d}{2} - 2l_{ev}\right) \\ &= \left(\frac{1}{3-1}\right)\left[\frac{16.0 \text{ in.}}{2} - 2(1\tfrac{1}{2} \text{ in.})\right] \\ &= 2\tfrac{1}{2} \text{ in.} \end{aligned}$$

The horizontal edge distance of the beam is:

$$5 \text{ in.} - 1\tfrac{1}{2} \text{ in.} - 0.4 \text{ in.} = 3.10 \text{ in.}$$

Step 3—Check the Beam Strength

Step 3a—Check for beam catenary action

The maximum moment in the beam (at mid-span) is determined using AISC *Manual* Table 3-23, Case 1:

$$\begin{aligned} \frac{wL^2}{8} &= \frac{(3 \text{ kip/ft})(20 \text{ ft})^2}{8} \\ &= 150 \text{ kip-ft} \end{aligned}$$

The beam elastic moment capacity is:

$$K_{yt}F_{yt}S_x = \frac{0.66(50\text{ ksi})(64.7\text{ in.}^3)}{12\text{ in./ft}}$$
$$= 178\text{ kip-ft} > 150\text{ kip-ft}$$

The beam will remain in the elastic zone; no catenary action will occur.

Step 3b—Check beam shear strength

The maximum shear applied on the beam (at the support) is determend using AISC *Manual* Table 3-23, Case 1:

$$V = \frac{wL}{2}$$
$$= \frac{(3\text{ kip/ft})(20\text{ ft})}{2}$$
$$= 30.0\text{ kips}$$

The shear yielding strength of the beam is determined as follows:

$$A_s = dt_w$$
$$= (16.0\text{ in.})(0.305\text{ in.})$$
$$= 4.88\text{ in.}^2$$

$$0.6K_{yt}F_{yt}A_s = 0.6(0.66)(50\text{ ksi})(4.88\text{ in.}^2)$$
$$= 96.6\text{ kips} > 30.0\text{ kips} \quad \textbf{o.k.}$$

Step 4—Determine the Forces on the Connection

Step 4a—Shear force on the connection due to gravity load

The shear force at the connection is determend using AISC *Manual* Table 3-23, Case 1:

$$V = \frac{wL}{2}$$
$$= \frac{(3\text{ kip/ft})(20\text{ ft})}{2}$$
$$= 30.0\text{ kips}$$

Step 4b—Compressive force on the connection due to thermal expansion of the beam

The coefficient of thermal expansion coefficient is:

$$\alpha = 1.2(10^{-5})/°\text{C}$$
$$= 6.67(10^{-6})/°\text{F}$$

The elongation of the beam due to thermal expansion is:

$$\Delta l = L(\Delta T)(\alpha)$$
$$= (20\text{ ft})(932°\text{F} - 68°\text{F})(6.67/°\text{F})(10^{-6})(12\text{ in./ft})$$
$$= 1.38\text{ in.}$$

Because the frame is symmetrical, the horizontal displacement of the column mid-span is:

$$\begin{aligned}\Delta &= \frac{\Delta l}{2}\\ &= \frac{1.38\text{ in.}}{2}\\ &= 0.690\text{ in.}\end{aligned}$$

The column temperature is roughly estimated to be 300°C (572°F) which is 60% of the beam temperature. From Table 3, the value of K_E at 300°C (572°F) is estimated at 0.90. Thus, the thermal compressive force applied to the connection is:

$$\Delta = \frac{PH^3}{48K_E EI_x}$$

Solving for P:

$$\begin{aligned}P &= \frac{48\Delta K_E EI_x}{H^3}\\ &= \frac{48(0.690\text{ in.})(0.90)(29{,}000\text{ ksi})(272\text{ in.}^4)}{(20\text{ ft})^3(12\text{ in/ft})^3}\\ &= 17.0\text{ kips}\end{aligned}$$

Step 4c—Moment applied at the connection

The beam line is a straight line that can be plotted from the moment and end rotation for a fixed-end beam and simply supported beam.

For a simply supported beam:

$$\begin{aligned}\theta_c &= \frac{wL^3}{24K_E EI_x}\\ &= \frac{(3\text{ kip/ft})(20\text{ ft})^3(12\text{ in./ft})^2}{24(0.771)(29{,}000\text{ ksi})(518\text{ in.}^4)}\\ &= 0.0124\text{ rad}\end{aligned}$$

$$M = 0\text{ kip-in.}$$

For a fixed-end beam:

$$\theta_c = 0\text{ rad}$$

$$\begin{aligned}M &= \frac{wL^2}{12}\\ &= \frac{(3\text{ kip/ft})(20\text{ ft})^2(12\text{ in./ft})}{12}\\ &= 1{,}220\text{ kip-in.}\end{aligned}$$

The beam-line and moment-rotation characteristics (using the stiffness model) of the connection are plotted in Figure 10. The moment applied to the connection is determined at the intersection of these two lines. Use M = 20.0 kip-in.

M is used to check the strength of the double-angle connection when subjected to beam-end moments.

Step 5—Compute the Applied Shear Force on the Bolts

The double angle is connected to the beam web by one column of three bolts.

Step 5a—Bolt shear force due to gravity load

$$
\begin{aligned}
V_v &= \frac{V}{n} \\
&= \frac{30.0 \text{ kips}}{3 \text{ bolts}} \\
&= 10.0 \text{ kips/bolt}
\end{aligned}
$$

Step 5b—Bolt shear force due to thermal expansion

$$
\begin{aligned}
V_p &= \frac{P}{n} \\
&= \frac{17.0 \text{ kips}}{3 \text{ bolts}} \\
&= 5.67 \text{ kips/bolt}
\end{aligned}
$$

Step 5c—Bolt shear force due to the applied moment on the connection

$$
\begin{aligned}
V_m &= \frac{M}{(n-1)s} \\
&= \frac{20.0 \text{ kip-in.}}{(3-1)(2\tfrac{1}{2} \text{ in.})} \\
&= 4.00 \text{ kips/bolt}
\end{aligned}
$$

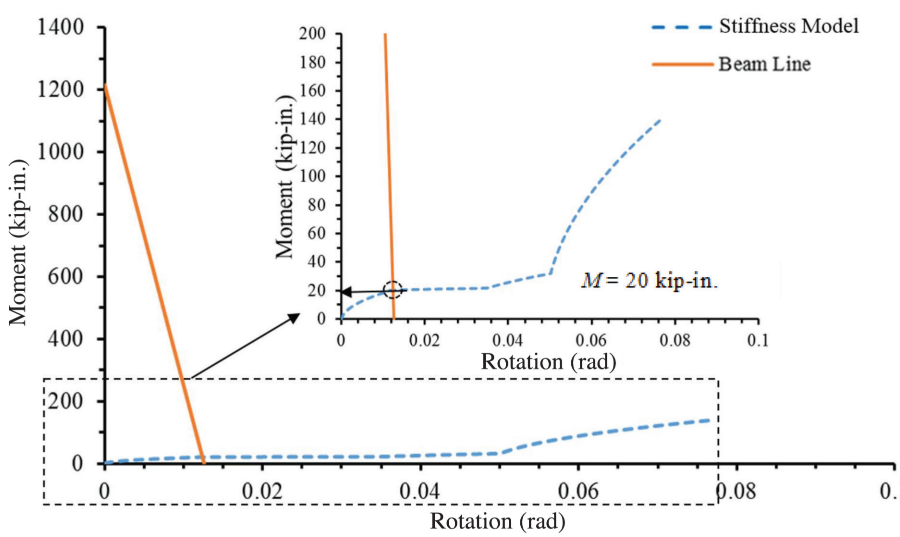

Fig. 10. Moment demand on the double-angle connection using beam-line theory.

Step 5d—Applied shear force on each bolt

$$
\begin{aligned}
V_{top} &= \sqrt{\left(V_m - V_p\right)^2 + \left(V_v\right)^2} \\
&= \sqrt{\left(4.00\text{ kips} - 5.67\text{ kips}\right)^2 + \left(10.0\text{ kips}\right)^2} \\
&= 10.1\text{ kips}
\end{aligned}
$$

$$
\begin{aligned}
V_{middle} &= \sqrt{\left(V_p\right)^2 + \left(V_v\right)^2} \\
&= \sqrt{\left(5.67\text{ kips}\right)^2 + \left(10.0\text{ kips}\right)^2} \\
&= 11.5\text{ kips}
\end{aligned}
$$

$$
\begin{aligned}
V_{bottom} &= \sqrt{\left(V_p + V_m\right)^2 + \left(V_v\right)^2} \\
&= \sqrt{\left(4.00\text{ kips} + 5.67\text{ kips}\right)^2 + \left(10.0\text{ kips}\right)^2} \\
&= 13.9\text{ kips}
\end{aligned}
$$

Step 5e—Applied axial force on each tension bolt (connecting the column to the angle)

The compression load applied on each bolt due to the beam thermal expansion is:

$$
\begin{aligned}
\frac{P}{6} &= \frac{17.0\text{ kips}}{6} \\
&= 2.83\text{ kips/bolt}
\end{aligned}
$$

To obtain the tension applied to the bolts due to the applied moment, the elastic method of distributing forces can be used. The moment applied on each angle is:

$$
\begin{aligned}
\frac{M}{2} &= \frac{20.0\text{ kip-in.}}{2} \\
&= 10.0\text{ kip-in.}
\end{aligned}
$$

For the system of angle leg in bearing and bolts in tension, the tension applied on the top bolt (critical bolt) due to M is:

$$
\begin{aligned}
P_m &= \frac{M}{2I_x} A_b p \\
&= \frac{10.0\text{ kip-in.}}{17.7\text{ in.}^4}\left(0.442\text{ in.}^2\right)\left(5.1\text{ in.}\right) \\
&= 1.27\text{ kips/bolt}
\end{aligned}
$$

$$
\begin{aligned}
P_{total} &= P_m - \frac{P}{6} \\
&= 1.27\text{ kips} - 2.83\text{ kips} \\
&= -1.56\text{ kips/bolt (compression)}
\end{aligned}
$$

Because all the bolts are in compression, there is no need to check the tensile bolt capacity (including prying effects), angle leg in bending, and bolt punching for the double angle.

Step 6—Determine the Angle Leg Strength

Shear applied on each angle leg is:

$$
\begin{aligned}
\frac{V}{2} &= \frac{30.0\text{ kips}}{2} \\
&= 15.0\text{ kips}
\end{aligned}
$$

The moment applied on each angle leg is:

$$\frac{M}{2} = \frac{20.0 \text{ kip-in.}}{2}$$
$$= 10.0 \text{ kip-in.}$$

Step 6a—Shear yielding

$$A_s = lt$$
$$= (8.00 \text{ in.})(3\!/\!8 \text{ in.})$$
$$= 3.00 \text{ in.}^2$$

$$R_{vy} = 0.6K_{yt}F_{yt}A_s$$
$$= 0.6(0.66)(50 \text{ ksi})(3.00 \text{ in.}^2)$$
$$= 59.4 \text{ kips} > 15.0 \text{ kips} \quad \textbf{o.k.}$$

Step 6b—Shear rupture

$$A_n = \left[l - n(d + 1\!/\!16 \text{ in.})\right]t_p$$
$$= \left[8.00 \text{ in.} - 3(13\!/\!16 \text{ in.} + 1\!/\!16 \text{ in.})\right](3\!/\!8 \text{ in.})$$
$$= 2.02 \text{ in.}^2$$

$$R_{vu} = 0.6K_{ut}F_{ut}A_n$$
$$= 0.6(0.64)(65 \text{ ksi})(2.02 \text{ in.}^2)$$
$$= 50.4 \text{ kips} > 15.0 \text{ kips} \quad \textbf{o.k.}$$

Step 6c—Flexural yielding

$$Z_x = \frac{t_p l^2}{4}$$
$$= \frac{(3\!/\!8 \text{ in.})(8.00 \text{ in.})^2}{4}$$
$$= 6.00 \text{ in.}^3$$

$$M_y = K_{yt}F_{yt}Z_x$$
$$= 0.66(50 \text{ ksi})(6.00 \text{ in.}^3)$$
$$= 198 \text{ kip-in.} > 10.0 \text{ kip-in.} \quad \textbf{o.k.}$$

Step 6d—Flexural rupture

The net plastic section modulus is not calculated here. Use $Z_{net} = 3.56$ in.^{3}

$$M_u = K_{ut}F_{ut}Z_{net}$$
$$= 0.64(65 \text{ ksi})(3.56 \text{ in.}^3)$$
$$= 148 \text{ kip-in.} > 10.0 \text{ kip-in.} \quad \textbf{o.k.}$$

Step 6e—Block shear rupture

$$R_n = 0.60A_{nv}K_{ut}F_{ut} + U_{bs}A_{nt}K_{ut}F_{ut} \le 0.60A_{gv}K_{yt}F_{yt} + U_{bs}A_{nt}K_{ut}F_{ut}$$

where

$$A_{nt} = \left[1\tfrac{1}{2}\text{ in.} - 0.5\left(\tfrac{13}{16}\text{ in.} + \tfrac{1}{16}\text{ in.}\right)\right]\left(\tfrac{3}{8}\text{ in.}\right)$$
$$= 0.398\text{ in.}^2$$

$$A_{gv} = \left(5.00\text{ in.} + 1\tfrac{1}{2}\text{ in.}\right)\left(\tfrac{3}{8}\text{ in.}\right)$$
$$= 2.44\text{ in.}^2$$

$$A_{nv} = \left[\left(5.00\text{ in.} + 1\tfrac{1}{2}\text{ in.}\right) - 2.5\left(\tfrac{13}{16}\text{ in.} + \tfrac{1}{16}\text{ in.}\right)\right]\left(\tfrac{3}{8}\text{ in.}\right)$$
$$= 1.62\text{ in.}^2$$

$$U_{bs} = 1.0$$

$$0.60A_{nv}K_{ut}F_{ut} = 0.60\left(1.62\text{ in.}^2\right)(0.64)(65\text{ ksi})$$
$$= 40.4\text{ kips}$$

$$0.60A_{gv}K_{yt}F_{yt} = 0.60\left(2.44\text{ in.}^2\right)(0.66)(50\text{ ksi})$$
$$= 48.3\text{ kips}$$

$$U_{bs}A_{nt}K_{ut}F_{ut} = 1.0\left(0.398\text{ in.}^2\right)(0.64)(65\text{ ksi})$$
$$= 16.6\text{ kips}$$

$$R_n = 0.60A_{nv}K_{ut}F_{ut} + U_{bs}A_{nt}K_{ut}F_{ut} \le 0.60A_{gv}K_{yt}F_{yt} + U_{bs}A_{nt}K_{ut}F_{ut}$$
$$= 40.4\text{ kips} + 16.6\text{ kips} < 48.3\text{ kips} + 16.6\text{ kips}$$
$$= 57.0\text{ kips} > 15.0\text{ kips} \quad \textbf{o.k.}$$

Step 7—Check Shear Transfer at Bolts

Step 7a—Bolt shear strength

$$R_v = 0.625nK_{bt}F_{ub}A_s(2)$$
$$= (0.625)(1)(0.379)(120\text{ ksi})\left[\frac{\pi\left(\tfrac{3}{4}\text{ in.}\right)^2}{4}\right](2)$$
$$= 25.1\text{ kips/bolt}$$

Step 7b—Angle leg bearing and tearout resistance

$$R_{br} = 3.0K_{ut}F_{ut}d_bt \le 1.5l_ctK_{ut}F_{ut}$$
$$= 3.0(0.64)(65\text{ ksi})\left(\tfrac{3}{4}\text{ in.}\right)\left(\tfrac{3}{8}\text{ in.}\right) \le 1.5(1.06\text{ in.})\left(\tfrac{3}{8}\text{ in.}\right)(0.64)(65\text{ ksi})$$
$$= 24.8\text{ kips/bolt per angle}$$

For the two angles:

$$2R_{br} = 2(24.8\text{ kips/bolt})$$
$$= 49.6\text{ kips/bolt}$$

Step 7c—Beam web bearing and tearout resistance

$$R_{br} = 3.0K_{ut}F_{ut}d_bt \le 1.5l_ctK_{ut}F_{ut}$$
$$= 3.0(0.64)(65\text{ ksi})\left(\tfrac{3}{4}\text{ in.}\right)(0.305\text{ in.}) \le 1.5(1.66\text{ in.})(0.305\text{ in.})(0.64)(65\text{ ksi})$$
$$= 28.5\text{ kips/bolt}$$

Table 4. Summary of the Limit State Available Strength for a Double-Angle Connection in Fire [500°C (932°F)]	
Mode	**Available Strength**
Shear yielding of angle leg =	59.4 kips
Shear rupture of angle leg =	50.4 kips
Flexural yielding of angle leg =	198 kip-in.
Flexural rupture of angle leg =	148 kip-in.
Block shear of angle leg =	57.0 kips
Bolt shear strength =	25.1 kips/bolt
Angle leg bearing and tearout strength =	24.8 kips/bolt
Beam web bearing and tearout strength =	28.5 kips/bolt

Comparing the strength of the bolts in shear to the angle leg and beam web in bearing and tearout, the bolt in shear has the minimum strength.

$$R_v = \min\{25.1 \text{ kips/bolt, } 49.6 \text{ kips/bolt, } 28.5 \text{ kips/bolt}\}$$
$$= 25.1 \text{ kips/bolt}$$

$$V_{top} = 10.1 \text{ kips} < 25.1 \text{ kips} \quad \textbf{o.k.}$$

$$V_{middle} = 11.5 \text{ kips} < 25.1 \text{ kips} \quad \textbf{o.k.}$$

$$V_{bottom} = 13.9 \text{ kips} < 25.1 \text{ kips} \quad \textbf{o.k.}$$

A summary of the limit state available strength is presented in Table 4. The designed connection can withstand the applied gravity loads at 500°C (932°F), in addition to the exerted moment by the beam on the connection and the compressive forces due to restrained thermal expansion. Further details of the final geometric configuration of the double-angle connection are given in Figure 11.

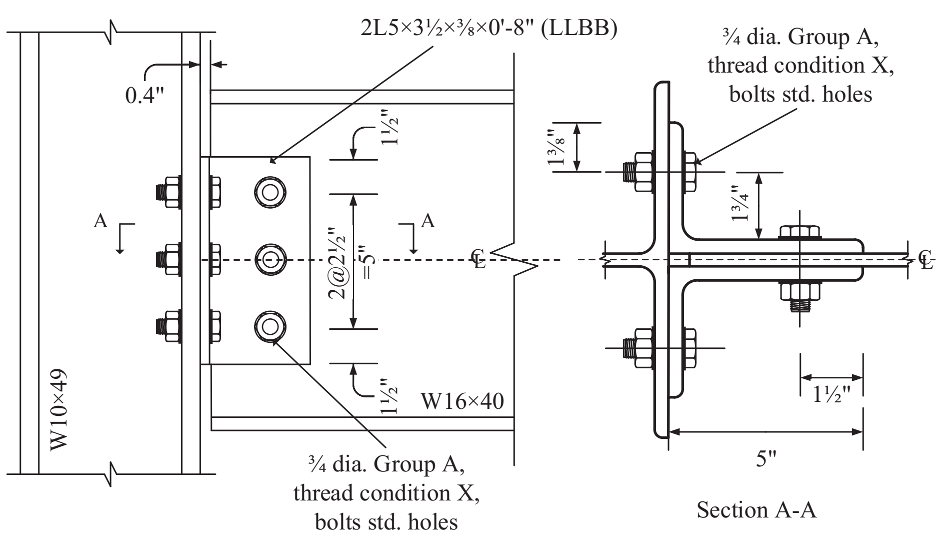

Fig. 11. Detailed design for W16×40 beam connected to W10×49 column through a double-angle connection.

CONCLUSIONS

The goal of this study is to propose fire design–oriented guidelines that aim at designing robust simple steel connections (shear tab and double angle) at low to medium temperatures of fire. To reach this aim, first, a simple tool, which can be used by professional structural fire engineers, is developed to characterize the stiffness and capacity of simple steel connections in fire. Thus, a stiffness-based model, which is considered to be a simple and practical tool, is proposed. The developed model is based on stiffness and strength equations available in the literature. Materials and geometric nonlinearities are incorporated in the proposed model to ensure accurate predictions of the connection response. Geometric nonlinearity can be observed through the complex interaction between connection components by surface to surface contact and slip of shear planes, whereas material nonlinearity is included through material yielding and steel retention factors. The proposed model is validated against experimental data available in the literature to test its prediction capabilities. It is able to capture—with reasonable accuracy—the force-rotation behavior of the connections when compared with the experimental results. Further, the ultimate capacities and failure modes from the experimental work results are identified and well predicted.

The study further incorporates the proposed stiffness model in fire design procedure of unprotected simple steel connections under transient-state conditions of fire. The design procedure is presented in two fire design examples illustrated as step-by-step design guidelines for simple steel connections. It accounts for the three main sources of stresses on the steel connections in fire: (1) the sustained gravity loads, (2) the induced axial load due to restrained thermal expansion, and (3) the moment demand exerted by the beam material (stiffness) degradation. Simplifications are identified and implemented to reach a simple and conservative design procedure to be used by professional structural fire engineers. Comparing the two design examples, it can be concluded that the double-angle connection exhibits a better performance than the shear tab connection when subjected to fire. The fact that the double-angle connection provides double shear planes to resist the applied loads, compared to one shear plane in the shear tab connection, makes it more flexible and resilient when subjected to fire. This is consistent with previous findings in the literature (Hantouche et al., 2016). Moreover, this study showed that the bolts are the most vulnerable element in the connection during fire, especially for shear tab connections with a single shear plane. This was also observed in the fire tests of Yu et al. (2009a, 2009c), where the failure mode was governed by shear bolt failure at high temperatures. This can be attributed to the severe reduction in the bolt ultimate strength (e.g., relatively low retention factor) when exposed to fire. Therefore, in such cases, it is advised to use A490-X bolts to increase the strength and ductility of simple steel connections. The bolts in steel connection should be given exceptional care in both design and construction phases.

This study should be extended to cover other aspects and load demands that the simple steel connections are subjected to at later stages (high temperatures) of fire—most importantly, tension stresses due to beam catenary action. Studies should be also conducted to ensure the survival of the connection during cooling phase where the connection is subjected to additional tension stresses. Moreover, the design of connections surrounded by a cooler structure in a full building system should be also considered. Creep material should be accounted for in the fire design to include the time-dependent effects. It is noteworthy that quite a bit of ongoing research is proving that steel connections and beams can survive fire events without having fire protection (insulation). These findings will eventually lead to establishing both safe and economic design of steel structures.

SYMBOLS

A_b	Effective area of the bolt shank, in.^{2}
A_f	Effective contact area of the beam, in.^{2}
A_{gv}	Gross area subject to shear for block shear failure mode, in.^{2}
A_{nt}	Net area subject to tension for block shear failure mode, in.^{2}
A_{nv}	Net area subject to shear for block shear failure mode, in.^{2}
A_s	Effective shear area (e.g. web area in beams), in.^{2}
A_{we}	Effective area of the weld, in.^{2}
D	Distance between the beam bottom flange and the center of rotation c, in.
D_u	Ratio of the mean installed bolt pretension to the specified minimum bolt pretension
E	Elastic modulus of steel material at ambient temperature, ksi
F_{EXX}	Filler metal classification strength at ambient temperature, ksi
F_{ub}	Ultimate strength of steel bolt at ambient temperature, ksi
F_{ut}	Ultimate strength of base material at ambient temperature, ksi
F_{yt}	Yield strength of base material at ambient temperature, ksi

H	Column height, ft
I_x	Moment of inertia about the x-axis, in.^{4}
K_E	Temperature-dependent retention factor for the elastic modulus of the base material
K_{bt}	Temperature-dependent retention factor for the ultimate strength of steel bolt
K_{ut}	Temperature-dependent retention factor the ultimate strength of the base material
K_{wt}	Temperature-dependent retention factor for the ultimate strength of the weld
K_{yt}	Temperature-dependent retention factor the yield strength of the base material
L	Length of the beam, ft
L_b	Elongation length of the bolt shank, in.
L_{eh}	Horizontal edge distance, in.
L_{ev}	Vertical edge distance, in.
M	Resultant moment on the connection calculated from applied shear and tensile forces, kip-in.
M_p	Plastic moment capacity, kip-in.
M_u	Rupture moment capacity, kip-in.
M_y	Yielding moment capacity, kip-in.
P	Axial force due to thermal expansion of the beam, kips
P_m	Axial force due to applied moment, kips
P_{total}	Total axial force, kips
R_b	Capacity of angle leg in bending, kips
R_{br}	Strength of plate/angle leg/beam web in bearing/tearout, kips
R_{bs}	Shear resistance of plate/angle leg against block shear, kips
R_{nw}	Weld strength, kips
R_{pn}	Shear resistance of plate/angle leg against bolt punching rupture, kips
R_s	Bolt slip resistance, kips
R_v	Bolt shear resistance, kips
R_{vu}	Shear resistance of plate/angle leg against shear rupture, kips
R_{vy}	Shear resistance of plate/angle leg against shear yielding, kips
R_t	Bolt tensile resistance, kips
S_x	Elastic section modulus about the x-axis, in.^{3}
T_b	Minimum pretension force applied on the bolt, kips
U_{bs}	Tension stress distribution factor
V	Applied shear force on the connection, kips
V_{bottom}	Applied shear force on the bottom bolt, kips
V_m	Bolt shear forces due to applied moment, kips
V_{middle}	Applied shear force on the middle bolt, kips
V_p	Bolt shear forces due to compressive force, kips
V_{top}	Applied shear force on the top bolt, kips
V_v	Bolt shear forces due to gravity load, kips
W	Applied uniformly distributed gravity load on the beam, kip/ft
Z_{net}	Net plastic section moduli about the x-axis, in.^{3}
Z_x	Plastic section moduli about the x-axis, in.^{3}
a	Distance from the bolt line to the weld line, in.
d_{M16}	Diameter of M16 bolt shank, in.
d_b	Diameter of bolt shank, in.
d_h	Diameter of bolt hole, in.
d_m	Mean of the across points and across flats dimensions of the bolt head or the nut, whichever is smaller, in.
e	Shear force eccentricity, in.
e_b	Distance from the bolt to the free edge of the plate in the direction of the load transfer, in.
f_t	Shear stress perpendicular and parallel to the weld line, ksi
f_v	Shear stress parallel to the weld line, ksi
h	Distance between the end components connecting shear tab/double angle to column, in.
h_f	Factor of fillers

k_{ab}	Stiffness of the web angle in bending, kip/in.
k_b	Parameter as defined in Equation 4
k_{bcc}	Stiffness of the beam flange in contact with the column, kip/in.
$k_{beam\text{-}angle\ lapjoint}$	Stiffness of a double-lap joint in double-angle connections, kip/in.
$k_{bolt\ row}$	Stiffness of a single bolt row, kip/in.
k_{bs}	Stiffness of the bolts in shear, kip/in.
k_{bt}	Stiffness of the bolts in tension, kip/in.
k_{pb}	Stiffness of beam web/angle leg in bearing, kip/in.
k_r	Rotational stiffness, kip-in.
k_r	Parameter as defined in Equation 5
k_{tb}	Stiffness of steel plates in bearing, kip/in.
l_c	Clear distance between the edge of the bolt hole and the edge of the material, in.
$l_{eff,ab}$	Effective length of the double angles in bending in each bolt-row, in.
m	Distance between the center of the bolt and the angle leg fillet, in.
n	Number of slip/shear planes
n_b	Number of bolt columns
p	Distance between the farthest bolt-row and center of rotation c, in.
p_b	Spacing of the bolt in the direction of the load transfer, in.
s	Setback distance, in.
s_{slip}	Sum of the gaps between the bolt shank and the edge of the bolt hole, in.
t	Thickness of shear tab plate, double-angle leg, or beam web, in.
Δ	Horizontal deflection at the mid-span of the column due to beam thermal expansion, in.
ΔT	Change in temperature, °F
Δl	Thermal elongation of the heated beam, in.
Ω	Temperature-dependent parameter defined by Yu et al. (2009c)
α	Coefficient of thermal expansion of steel, °F
θ	Angle between the line of action of the required force and the weld longitudinal axis, degrees
θ_c	Connection rotation, rad
$\theta_{beam\text{-}contact}$	Angle of contact between the beam flange and the column flange, rad
$\theta_{bolt\text{-}contact}$	Angle at which the farthest bolt comes in contact with respective bolt hole edge, rad
μ	Mean slip coefficient

ACKNOWLEDGMENTS

The authors gratefully acknowledge the financial support provided by the American University of Beirut Research Board under grant No. 103604-24705. The authors further would like to thank the researchers at the University of Sheffield for making the connection test results publicly available.

REFERENCES

AISC (2016), *Specification for Structural Steel Buildings*, ANSI/AISC 360-16, American Institute of Steel Construction, Chicago, Ill.

AISC (2017), *Steel Construction Manual*, 15th Ed., American Institute of Steel Construction, Chicago, Ill.

CEN (2005a), *Eurocode 3: Design of Steel Structures—Part 1–2: General Rules—Structural Fire Design*, European Committee for Standardization, Brussels.

CEN (2005b), *Eurocode 3: Design of Steel Structures—Part 1–8: Design of Joints*, European Committee for Standardization, Brussels.

Garlock, M.E. and Selamet, S. (2010), "Modeling and Behavior of Steel Plate Connections Subject to Various Fire Scenarios," *Journal of Structural Engineering*, ASCE, Vol. 136, No. 7, pp. 897–906.

Hantouche, E.G., Abboud, N.H., Morovat, M.A., and Engelhardt, M.D. (2016), "Analysis of Steel Bolted Double Angle Connections at Elevated Temperatures," *Fire Safety Journal*, Vol. 83, pp. 79–89.

Hu, G. and Engelhardt, M. (2012), "Studies on the Behavior of Steel Single-Plate Beam End Connections in a Fire," *Structural Engineering International*, Vol. 22, No. 4, pp. 462–469.

Hu, Y., Davison, J.B., Burgess, I.W., and Plank, R.J. (2007), "Comparative Study of the Behaviour of BS 4190 and BS EN ISO 4014 Bolts in Fire," *Proceedings, 3rd International Conference on Steel and Composite Structures*, Taylor & Francis, Manchester, England, pp. 587–592.

Lee, J., Morovat, M.A., Hu, G., Engelhardt, M.D., and Taleff, E. (2013), “Experimental Investigation of Mechanical Properties of ASTM A992 Steel at Elevated Temperatures,” *Engineering Journal*, AISC, Vol. 50, No. 4, pp. 249–272.

Pakala, P., Kodur, V., Selamet, S., and Garlock, M. (2012), “Fire Behavior of Shear Angle Connections in a Restrained Steel Frame,” *Journal of Constructional Steel Research*, Vol. 77, pp. 119–130.

Seif, M., Main, J., Weigand, J., McAllister, T.P., and Luecke, W. (2016), “Finite Element Modeling of Structural Steel Component Failure at Elevated Temperatures,” *Structures*, Vol. 6, pp. 134–145.

Seif, M.S., Main, J.A., and McAllister, T.P. (2013), “Performance of Steel Shear Tab Connections at Elevated Temperatures,” *Proceedings of the Annual Stability Conference*, *Structural Stability Research Council*, St. Louis, Mo., pp. 16–20.

Selamet, S., and Garlock, M.E. (2010), “Robust Fire Design of Single Plate Shear Connections,” *Engineering Structures*, Vol. 32, pp. 2,367–2,378.

Sunder, S. (2005), “Final Report on the Collapse of the World Trade Center Towers: Federal Building and Fire Safety Investigation of the World Trade Center Disaster,” National Institute of Standards and Technology.

University of Sheffield (2007), EPSRC Project EP/C510984/1: Robustness of Joints in Fire, 2005–2008, http://fire-research.group.shef.ac.uk/downloads.html.

Wald, F., Simões da Silva, L., Moore, D.B., Lennon, T., Chladná, M., Santiago, A., Beneš, M., and Borges, L. (2006), “Experimental Behaviour of a Steel Structure under Natural Fire,” *Fire Safety Journal*, Vol. 41, No. 7, pp. 509–522.

Wang, Y.C., Dai, X.H., and Bailey, C.G. (2011), “An Experimental Study of Relative Structural Fire Behaviour and Robustness of Different Types of Steel Joint in Restrained Steel Frames,” *Journal of Constructional Steel Research*, Vol. 67, No. 7, pp. 1,149–1,163.

Wuwer, W., Zamorowski, J., and Swierczyna, S. (2012), “Lap Joints Stiffness According to Eurocode EC3 and Experimental Investigations Results,” *Archives of Civil and Mechanical Engineering*, Vol. 12, No. 1, pp. 95–104.

Yu, H., Burgess, I.W., Davison, J.B., and Plank, R.J. (2009a), “Tying Capacity of Web Cleat Connections in Fire, Part 1: Test and Finite Element Simulation,” *Engineering Structures*, Vol. 31, No. 3, pp. 651–663.

Yu, H., Burgess, I.W., Davison, J.B., and Plank, R.J. (2009b), “Tying Capacity of Web Cleat Connections in Fire, Part 2: Development of Component-Based Model,” *Engineering Structures*, Vol. 31, No. 3, pp. 697–708.

Yu, H., Burgess, I.W., Davison, J.B., and Plank, R.J. (2009c), “Experimental Investigation of The Behaviour of Fin Plate Connections in Fire,” *Journal of Constructional Steel Research*, Vol. 65, No. 3, pp. 723–736.

Zhang, C., and Usmani, A. (2015), “Heat Transfer Principles in Thermal Calculation of Structures in Fire,” *Fire Safety Journal*, Vol. 78, pp. 85–95.